

1 Formaldehyde (HCHO) in air, snow and interstitial air at Concordia (East Antarctic plateau)  
2 in summer

3  
4 Susanne Preunkert<sup>1,2</sup>, Michel Legrand<sup>1,2</sup>, Markus Frey<sup>3</sup>, Alexandre Kukui<sup>4,5</sup>, Joel Savarino<sup>1,2</sup>,  
5 Hubert Gallée<sup>1,2</sup>, Martin King<sup>6</sup>, Bruno Jourdain<sup>1,2</sup>, William Vicars<sup>7</sup>, and Detlev Helmig<sup>7</sup>

6  
7 <sup>1</sup> CNRS, Laboratoire de Glaciologie et Géophysique de l'Environnement (LGGE), F-38000  
8 Grenoble,

9 <sup>2</sup>Univ. Grenoble Alpes, LGGE, F-38000 Grenoble, France

10 <sup>3</sup> British Antarctic Survey (BAS), Natural Environment Research Council, Cambridge, UK

11 <sup>4</sup> Laboratoire des Atmosphères, Milieux, Observations Spatiales (LATMOS), Paris, France

12 <sup>5</sup> Laboratoire de Physique et Chimie de l'Environnement et de l'Espace (LPC2E) UMR-  
13 CNRS, Orléans, France

14 <sup>6</sup> Department of Earth Sciences, Royal Holloway University of London, Egham, Surrey,  
15 TW20 0EX, UK

16 <sup>7</sup> Institute of Arctic and Alpine Research (INSTAAR), University of Colorado, Boulder

17  
18  
19  
20 Correspondence email: [Preunkert@lgge.obs.ujf-grenoble.fr](mailto:Preunkert@lgge.obs.ujf-grenoble.fr)  
21  
22

#### Abstract

During the 2011/12 and 2012/13 austral summers HCHO was investigated for the first time in ambient air, snow, and interstitial air at the Concordia site located near Dome C on the East Antarctic plateau by deploying an Aerolaser AL-4021 analyser. Snow emission fluxes were estimated from vertical gradients of mixing ratios observed at 1 cm and 1 m above the snow surface as well as in interstitial air a few cm below the surface and in air just above the snow-pack. Typical flux values range between 1 to  $2 \times 10^{12}$  molecules  $\text{m}^{-2} \text{s}^{-1}$  at night and 3 to  $5 \times 10^{12}$  molecules  $\text{m}^{-2} \text{s}^{-1}$  at noon. Shading experiments suggest that the photochemical HCHO production in the snowpack at Concordia remains negligible compared to temperature-driven air-snow exchanges. At 1 m above the snow surface, the observed mean mixing ratio of 130 pptv and its diurnal cycle characterized by a slight decrease around noon are quite well reproduced by 1-D simulations that include snow emissions and gas phase methane oxidation chemistry. Simulations indicate that the gas-phase production from  $\text{CH}_4$  oxidation largely contributes (66%) to the observed HCHO mixing ratios. In addition, HCHO snow emissions account for  $\sim 30\%$  at night and  $\sim 10\%$  at noon to the observed HCHO levels.

## 1. Introduction

Over continents, formaldehyde is produced within the atmosphere during the oxidation of numerous hydrocarbons emitted by anthropogenic and natural sources and also directly emitted by combustion. In the remote marine troposphere, HCHO is thought to be mainly produced by the photo-oxidation of CH<sub>4</sub>, the most abundant atmospheric hydrocarbon (Lowe and Schmidt, 1983). In addition to wet and dry deposition, the main sinks of HCHO are photolysis and reaction with OH leading to a typical HCHO atmospheric lifetime of a few hours (Seinfeld and Pandis, 2006).

At remote high-latitude sites several studies were conducted over the Arctic and Antarctic snowpack to evaluate the importance of the snowpack as a formaldehyde source for the atmospheric polar boundary layer (Sumner and Shepson, 1999; Yang et al., 2002; Jacobi et al., 2002; Hutterli et al., 2004; Riedel et al., 1999; Salmon et al., 2008). The understanding of the budget of HCHO in polar region is of importance since HCHO represents an important source of RO<sub>2</sub> radicals in the remote polar atmosphere, and is therefore intimately linked to the oxidative capacity of the atmosphere in these regions. This is true in margin regions of Antarctica as concluded on the basis of examinations of the observed HO<sub>x</sub> budgets at Halley (Bloss et al., 2007) and Dumont d'Urville (DDU, Kukui et al., 2012). At these two coastal sites, the HCHO budget was recently discussed by Preunkert et al. (2013), who concluded that, depending on the oxidative character of the local atmosphere and on the thickness and stability of the atmospheric boundary layer, either the methane oxidation by OH followed by reaction with NO, or snow emissions from neighbouring snow covered regions dominate the HCHO budget. At DDU the largest HCHO source is the methane oxidation in relation with a level of oxidants 3 times higher compared to Halley, and more frequent air mass transport from inland Antarctica there. At Halley, the shallower boundary layer makes snow emissions the dominant HCHO source. The examination of the observed HO<sub>x</sub> budget at the South Pole (Chen et al., 2004) and Concordia (Kukui et al., 2014) pointed out the role of HCHO on the RO<sub>2</sub> budget over the Antarctic plateau. At the South Pole, Hutterli et al. (2004) quantified snow-air fluxes on the basis of both atmospheric vertical gradients and firn air measurements. It has to be emphasized that the South Pole remains up to now the single Antarctic site where such a direct quantification of snow HCHO emissions was done.

The aims of the present study are (1) to document the boundary layer HCHO mixing ratio at Concordia during the OPALE (Oxidant Production over Antarctic Land and its Export) project (Preunkert et al., 2012) (see also Kukui et al., 2014), (2) to quantify the

summer HCHO snow emissions under conditions encountered at day and night at Concordia, and (3) to compare the role of snow emissions with that of the gas-phase production of HCHO in central Antarctica.

## **2. Methods and Field Campaigns**

Data presented in this study were obtained during two summer field campaigns having taken place at Concordia located on the high East Antarctic plateau (75°06'S, 123°33'E). The 2011/12 campaign conducted from late November 2011 to mid-January 2012 (i.e., the second OPALE field campaign) was mainly dedicated to document HCHO levels at two different heights in the air above the snow surface and to do a few HCHO measurements in interstitial air and in snow. During the 2012/13 campaign (December 22<sup>nd</sup> 2012 to January 25<sup>th</sup> 2013) HCHO was measured at different heights in air and firn in the framework of the snow tower experiment SUNITEDC (Evolution du Sulfate et du Nitrate de l'air et de la neige de Dôme C). Hereby the priority was to gain a detailed picture of the HCHO distribution in the interstitial air of the snowpack.

In the following section we first describe the analytical method used to measure HCHO. Then, for each campaign we present on site measurement set up and applied working conditions, as well as achieved detection limits in air, interstitial air and snow (Sect. 2.2 and 2.3). Finally, the model used to discuss the different source contributions to the atmospheric HCHO budget at Concordia are briefly introduced in Sect. 2.4.

### **2.1 Analytical method**

HCHO measurements were performed using a commercial Aerolaser analyzer (AL-4021). The technique, a continuous liquid fluorimetry, has been described in detail elsewhere (Dasgupta et al., 1988). Gaseous HCHO is scrubbed into a diluted sulfuric acid solution followed by reaction with the Hantzsch reagent, a dilute mixture of acetyl acetone, acetic acid, and ammonium acetate. Aqueous-phase formaldehyde reacts with the Hantzsch reagent to produce a fluorescent compound that is detected at 510 nm. The working conditions applied to the AL 4021 deployed at Concordia were similar to those applied by Preunkert et al. (2013) in their study conducted at the coastal Antarctic site of Dumont D'Urville. In brief, raw data are monitored with a time resolution of 30 s, gas standard calibration and zero determinations are made every 12 h and 2 h, respectively. While Preunkert et al. (2013) used an air flow of 2 L STP min<sup>-1</sup> (leading to a stripping efficiency of 98%) in view to obtain accurate HCHO measurements of the low winter levels encountered at DDU, the flow rate

was set here when possible (see Sect. 2.3) to 1 L STP min<sup>-1</sup>, as recommended by Aerolaser company, to reach a stripping efficiency of more than 99% (M. Haaks, personal communication 2011). As discussed by Preunkert et al. (2013), to minimize effects of changing temperatures in the laboratory at Concordia, the monitor was run in a box that was thermostated at 20°C.

## 2.2 The 2011/12 Field Experiments

Atmospheric HCHO was measured at 1 m (Fig. 1a) and 1 cm (not shown) above the snow surface at a place located ~ 900 m south-southwest from the main station from late November 2011 to mid-January 2012. Two 15 m long PTFE tubes (4 mm internal diameter) were used to bring ambient air sampled at the two heights into the field laboratory. Through the tubes, air was sucked with an external pump at a flow rate of 4 to 6 L min<sup>-1</sup> to keep its residence time in the lines low enough to maintain potential losses below 5 % (see details in Preunkert et al., 2013). To avoid condensation, the airlines were heated. In turn of 15 min the air inlet of the AL-4021 is connected to these tubes via a 50 cm long PTFE tube (internal diameter 4 mm) and a PTFE coated 3-way electro valve. The tightness of the sampling line was regularly controlled. Comparison of the two 15 m long airlines made by putting their air entries at the same height (1 m) showed no systematic differences (mean difference of  $2.5 \pm 40$  pptv over 10 h).

The detection limit of the analyzer calculated as twice the standard deviation of raw data (30 s) obtained during the 25 min zero measurements, which were made every 2 hours, is reported in Fig. 1b. Over the first two weeks of the sampling period, the detection limit remained low and similar to what was observed with the same analyzer (~ 30 pptv) during the year-round study conducted at DDU by Preunkert et al. (2013). During the second half of the sampling period at Concordia, the detection limit was enhanced exceeding 100 pptv on December 30<sup>th</sup>, due to a recurrent presence of air bubbles in the analyzer.

HCHO measurements started on December 14<sup>th</sup> but were interrupted several times after January 3<sup>rd</sup> due to problems with the fluorimeter of the AL-4021 (see Fig.1 for data availability). During the sampling period, no significant snowfall event took place and the main wind direction was from the southeast to southwest. However, several episodes (spanning 18% of the total time) with wind blowing from North (from 30°W to 60°E sector, i.e. the direction of the station) were encountered (Fig. 1c). Two major North wind periods took place from December 30<sup>th</sup> to January 1<sup>st</sup> in the morning and most of time after January 9<sup>th</sup> (Fig. 1c). Since during these events, scattered HCHO values were often observed we

cannot exclude a contamination from the station, and therefore the corresponding values were removed from the data set (see red points in Fig. 1a).

Due to either the presence of air bubbles in the analyzer, leading to a detection limit well above 30 pptv, or to scattered values related to contamination from station activities, qualified data on atmospheric HCHO at 1 cm and 1 m above the snow surface (see Sect. 4) are limited to the period of December 14<sup>th</sup> to December 28<sup>th</sup>. Anyway, note that the HCHO mixing ratio at 1 m ( $131 \pm 45$  pptv calculated with the few data available between January 1<sup>st</sup> and January 11<sup>th</sup>, see the horizontal dashed line in Fig. 1a) remains similar to the mean value of  $127 \pm 31$  pptv observed between December 14<sup>th</sup> and December 28<sup>th</sup>.

During the 2011/12 campaign, interstitial air was sampled in the snow between 5 and 100 cm depth by using a custom built firn air probe (a tube of 10 cm diameter described in Frey et al., this issue) (see Sect. 4.2). The probe was lowered vertically into a pre-cored hole to different snow depths, passing through a disc of 1 m diameter equipped with a lip of 10 cm, which was resting on the snow surface to limit preferential pumping of ambient air along the tube walls. All probe components were made from UV-transparent Plexiglas. In spite of exposition of the firn probe to Antarctic sunlight over the whole summer 2009/10, a contamination up to some 1000 pptv at the beginning of the field season coming either from the Plexiglas itself and/or from the glue used to assemble the different parts of the probe was detected in firn air. In addition, with values of up to a few ppbw (parts per billion by weight) the snow located between the surface and 20 cm depth around the firn probe was also contaminated. At the end of the season, the contamination of firn air became quasi insignificant as suggested by the observed HCHO values at that time (400 pptv at a depth of 10 cm) that are far lower than those observed at the beginning of the campaign and are in good agreement with those obtained during the 2012/13 campaign. Thus, it was possible to use the device to investigate the influence of UV-radiations on HCHO levels in firn air. This was done January 11<sup>th</sup> from 10:00 LT to 18:00 LT by placing UV-filters (2 x 3 m sheets of UV-opaque Plexiglas, Acrylite OP-3) at 1 m above the snow surface. In order to separate radiative and temperature effects, these filters were alternatively exchanged with sheets of UV-transparent Plexiglas (Acrylite OP-4).

Surface snow and snow pit samples were analyzed to document the bulk HCHO content at Concordia. Twenty meters away from the place where the HCHO firn measurements were done, the skin layer (the uppermost cm) of the snowpack was sampled 6 times on December 26<sup>th</sup> and December 27<sup>th</sup>, 26 times from January 2<sup>nd</sup> to 4<sup>th</sup>. In addition, 20 snow-pit samples were collected down to 70 cm depth on December 27<sup>th</sup>. Another snow-pit was dug January 9<sup>th</sup>

at 3 km from the main station and sampled down to 110 cm depth (21 samples). To avoid contamination, samples were collected in airtight Schott glass bottles (Legrand et al., 2007) and analyzed on site within a few hours after sampling. For these measurements the AL-4021 was run in liquid mode using 6 liquid standards containing from 0 to 6 ppbw of HCHO, which were freshly prepared by diluting a certified stock solution of 0.3 g L<sup>-1</sup> (purchased from the University of Wuppertal, Germany). Under these conditions a detection limit as low as 0.1 ppbw is achieved (Legrand et al., 2007). In addition, snow samples were also analyzed for cations and anions following ion chromatography working conditions reported in Legrand et al. (2013).

### 2.3 The 2012/13 Field Experiments

HCHO was measured from December 22<sup>nd</sup> 2012 to January 25<sup>th</sup> 2013 at different heights in air and firn, about 800 m west from the main station in the clean area sector. During this period no important precipitation occurred and wind never blew from 70°E to 110°E (i.e. from the direction of the station). Snow temperatures were measured at different depths by using type-E thermocouples (Omega Engineering).

The principle of the snow tower experiment is detailed in Soek et al. (2009) and Helmig et al. (2007). In brief, three towers (one meteorological tower, MT, and two snow towers, ST1 and ST2) were installed in a distance of ~15 m to sample air above and below the snow surface. In this paper we report on HCHO data gained on the MT and ST2. Air was sampled from the MT at around 11 m, 2 m and 0.3 m above the surface at a flow rate of 5 L min<sup>-1</sup>. To avoid collection of ice crystals, each line was equipped with a PFA inlet funnel with 1 mm grids and 1 µm Teflon membrane filters (Savillex Co., USA). On the ST, air is sampled at 20 cm above the snow surface, just at the surface (0 cm), and at 20, 40, 60, and 80 cm below the surface. Air was drawn through each paired inlet of ST2 for 10 min (at ~1 L min<sup>-1</sup>) in turn of 2 h. Applying the calculations made in Soek et al. (2009) for DC conditions, 100% of sampled interstitial air would correspond to the height of the inlet ± 16 cm, and 66% to the height of the inlet ± 7 cm. That avoids significant overlapping with the adjacent inlets. For a given depth, the time between two subsequent samplings (2h) is more than twice the time needed for air under DC conditions to re-equilibrate to its original conditions (see calculations made in Soek et al., 2009). 25 mm Acrodisc hydrophobic PTFE syringe filters (Pall Life Sciences) previously passivized with O<sub>3</sub> were placed at all ST inlets to protect them from ice crystals.

During the campaign, sampled air was provided to the AL-4021 and to each of the other running analyzers ( $\text{NO}_x$ , Hg, and CO, not discussed here), with a flow rate of  $1 \text{ L min}^{-1}$  (i.e.  $0.7 \text{ L STP min}^{-1}$ ). Therefore, the airflow of the AL-4021 was set to  $0.6 \text{ L STP min}^{-1}$  what is 40% lower than the one normally applied for the AL-4021 (see Sect. 2.1), resulting in an ~25% lower sensibility of the instrument. Taken as twice the standard deviation of zero measurements, the detection limit was  $67 \pm 22 \text{ pptv}$  from December 22<sup>nd</sup> to January 6<sup>th</sup> (151 zero measurements) and  $120 \pm 55 \text{ pptv}$  from January 6<sup>th</sup> to 25<sup>th</sup> (185 zero measurements). Compared to other experiments performed with the device (see Sect. 2.2) these rather high detection limits were due related to a frequent presence of air bubbles in the analyzer lines. Twice per week, the inlets of the 3 MT lines were placed for 1 hour at 2 m height, showing no systematic differences ( $4 \pm 21 \text{ pptv}$  and  $5 \pm 29 \text{ pptv}$  with respect to one inlet reference). Such a comparison of the different airlines was not possible for ST2 since HCHO measurements started well after their set up in snow.

As seen in Fig. 2a, overall means of HCHO air mixing ratios measured at MT through the 11 m, 2 m and 0.3 m inlets are  $164 \pm 55 \text{ pptv}$ ,  $168 \pm 54 \text{ pptv}$  and  $170 \pm 61 \text{ pptv}$ , respectively. The mean value observed at 20 cm above the snow surface at ST2 is  $203 \pm 55 \text{ pptv}$ . From December 20<sup>th</sup> to 22<sup>nd</sup>, HCHO was sampled at 20 cm above the surface by using a 3 m long PTFE line (internal diameter 4 mm) connected directly to the AL-4021, giving a mixing ratio of  $135 \pm 48 \text{ pptv}$ . In view of the high variability encountered for HCHO measurements during this experiment, these values show no significant difference. However, the relative high mean atmospheric HCHO mixing ratios measured at ST2 might be also related to the fact that ST air lines were not flushed continuously but only for 10 min each 2 h. Given these enhanced measurement uncertainties, absolute atmospheric HCHO mixing ratios are not investigated within this 2012/13 data set, but the measurements will be used to examine HCHO in interstitial air (see Sect. 4.2), in view to derive HCHO fluxes between the snow pack and the atmosphere (Sect. 5.2) and to discuss its firn-air equilibrium (Sect. 5.3).

## 2.4 Model calculations

Observed HCHO mixing ratios (daily mean and diurnal variation) were compared with those simulated by a 1-D box model that considers snow HCHO emissions as well as the local gas-phase photochemistry.

Input parameters used in the model were gained from on site atmospheric measurements made during the 2011/12 experiment which included  $\text{NO}$ ,  $\text{OH}$ ,  $\text{RO}_2$ , and



1 methylhydroperoxide (MHP). NO was determined with a 2-channel chemiluminescence  
2 detector following working conditions detailed in Frey et al. (2013) and Frey et al. (this issue)  
3 The OH and RO<sub>2</sub> radicals were measured using chemical ionisation mass spectrometry  
4 (Kukui et al., 2012; Kukui et al., 2014). During the campaign the photolysis rates of HCHO  
5 were documented using a 2 $\pi$  spectroradiometer (Metcon company). MHP was measured  
6 together with H<sub>2</sub>O<sub>2</sub> deploying an Aerolaser AL-2021 instrument as during the first OPALE  
7 campaign conducted at DDU (Preunkert et al., 2012).

8 For snow emissions, we used values derived from the observed vertical gradient  
9 between 1 cm and 1 m above the snow surface as well as those derived from the observed  
10 difference between snow interstitial air and air above the snow surface (see Sect. 5). For  
11 calculations of the gas phase photochemistry we considered the model used by Preunkert et  
12 al. (2013) to examine the budget of HCHO at the Antarctic coast that includes the CH<sub>4</sub>  
13 oxidation as well as the oxidation of non-methane hydrocarbons (light alkenes and DMS)  
14 together with major sinks of HCHO (its photolysis and reaction with OH). For simulations at  
15 Concordia, we neglected the oxidation of ethene and DMS oxidation pathways. Indeed, even  
16 with a DMS summer mixing ratio of 50 pptv at DDU (against less than 1 pptv at Concordia,  
17 Preunkert et al., 2008), and an ethene level of 17 pptv (against less than 3 pptv expected for  
18 Concordia as measured at South Pole, Beyersdorf et al., 2010), Preunkert et al. (2013)  
19 concluded that the gas phase production of HCHO from DMS and non-methane hydrocarbons  
20 only represents a few percent of the gas phase production (i.e. ~ 4%) dominated by the  
21 methane oxidation. The 15 gas-phase reactions considered in this work (see Table 1) will also  
22 permit to evaluate the influence of the bromine chemistry.

23 The vertical transport of the 1-D model was represented using vertical distribution of  
24 turbulent diffusion coefficients (K<sub>z</sub>) calculated by the regional atmospheric MAR model  
25 (Modèle Atmosphérique Régional). More details of MAR and of its reliability at Concordia  
26 during the OPALE campaign are given in Gallée and Gorodetskaya (2008) and Gallée et al.  
27 (this issue). Similarly to calculations performed by Legrand et al. (2014), we used the MAR  
28 data obtained with a horizontal resolution of 20 km centered at Concordia, a vertical  
29 resolution of 0.9 m for the height of up to 23 m above the surface decreasing upward to about  
30 50 m at the height of 500 m and to ~ 1800 m at the top level of ~ 24 km. For the 1D model,  
31 the K<sub>z</sub> values were linearly interpolated to the vertical 1D grid which was 0.1m from the  
32 surface to 5 m, 0.2 m from 5 to 7 m, 0.5 m from 7 to 10 m, around 1 m from 10 to 20 m, and  
33 then increases up to 120 m at 1200 m, the top height of the 1D model. Note that, the planetary  
34 boundary layer (PBL) height, defined by MAR as the height where the turbulent kinetic

energy decreases below the value at the lowest layer of the model, was always lower than the top layer of the 1D model during the OPALE campaign.

Since cloud cover is responsible for an increase of around 50% of the down-welling long-wave radiations in summer at DC, but the MAR model underestimates cloud cover, the surface heat budget is not well simulated during overcast days and this strongly impacts the turbulence simulated by the model. We therefore performed calculations only for days with clear sky conditions.

### **3. Ambient air HCHO mixing ratio at Concordia in summer 2011/12**

At Concordia, atmospheric HCHO levels remained close to  $130 \pm 37$  pptv from mid December 2011 to mid January 2012. Though underlying an enhanced variability, atmospheric HCHO mixing ratios measured from mid December 2012 to end of January 2013 (see Sect. 2.3) seem also to be free of important fluctuations. These quite constant HCHO mixing ratios contrast with observations made at South Pole, where fast HCHO decreases were observed during fog events (up to 100 pptv, Hutterli et al., 2004). At Concordia, the regular appearance of diamond dusts during early morning does not seem to disturb the daily course of the HCHO level (Fig. 3).

The HCHO level of 130 pptv observed at Concordia is consistent with those observed by Frey et al. (2005) at South Pole and Byrd Station (Table 2). For South Pole, the mean value reported for 16 days by Hutterli et al. (2004) is lower than the one observed by Frey et al. (2005) over 3 days (103 pptv instead of 155 pptv). However, during the period covered by measurements, Hutterli et al. (2004) experienced 3 days with values close to 50 pptv, corresponding to fog events that depleted HCHO in the boundary layer. Discarding these 3 days a mean value of 111-115 pptv is calculated. Note also that these values observed inland Antarctica remain in the same order as the ones reported at the coast (Table 2), for which Preunkert et al. (2013) discussed major sources (methane oxidation and snow emissions) and sinks (photolysis, destruction by OH, and dry deposition). The contribution of these different processes on the atmospheric HCHO budget at Concordia will be quantified in Sect. 6.

The daily course of atmospheric HCHO mixing ratios is reported in Fig. 3. We here removed data gained during overcast weather (see Fig.1) to make the data consistent with simulations made in Sect. 6 since the PBL height from the MAR model is significantly improved under clear sky conditions. We have examined separately data gained over two periods (from December 14<sup>th</sup> to 18<sup>th</sup> and December 19<sup>th</sup> to 28<sup>th</sup>) in view of the significant rise of the temperature between December 18<sup>th</sup> and 19<sup>th</sup> (Fig. 1d). In spite of this change of

temperature, the mean HCHO mixing ratios remained similar over the two periods (124 pptv from December 14<sup>th</sup> to 18<sup>th</sup> and 128 pptv from December 19<sup>th</sup> to 28<sup>th</sup>). Since enhanced temperatures are expected to increase HCHO snow emissions (Hutterli et al., 2002; Barret et al., 2011a), and given the decrease of the PBL height from prior to after December 19<sup>th</sup>, rather unchanged HCHO mixing ratios would suggest that snow emissions control only weakly the HCHO budget of the atmospheric boundary layer at Concordia. This point will be further discussed in Sect. 6.

From December 14<sup>th</sup> to 18<sup>th</sup>, only a small day/night difference of HCHO values can be observed with slightly lower daytime values (116 pptv between 8:00 LT and 14:00 LT) than nighttime values (126 pptv between 15:00 LT and 7:00 LT). During the following period (December 19<sup>th</sup> to 28<sup>th</sup>) when air temperatures were enhanced, a marked daily cycle (amplitude close to 30 pptv) characterized by a broad minimum from 7:00 LT to 15:00 LT and a broad maximum from 16:00 LT to 6:00 LT is observed.

## **4. HCHO in the snowpack**

### **4.1 HCHO in snow**

Fig. 4a shows the bulk snow HCHO profiles obtained in the two snow-pits dug at Concordia during the 2011/12 campaign (Sect. 2.2). The good agreement of data between the snow-pit dug December 27<sup>th</sup> near the air sampling site and the January 9<sup>th</sup> one dug at 3 km from the station suggests that station activities had little impact on the HCHO content of the snowpack in the immediate vicinity of the station. Note that the two profiles are also in good agreement with the one made by Hutterli et al. (2002) in January 1998 (i.e. well before the start in 2003 of overwintering station activities at Concordia).

The three depth profiles show a similar decreasing trend with depth reaching a value of 0.2-0.3 ppbw below 70 cm depth. Some differences exist between the three profiles with a maximum of 1 ppbw measured by Hutterli et al. (2002) at the surface against lower values in this study. Indeed, with individual values ranging from 0.2 to 0.4 ppbw, the 26 skin layer snow samples (Sect. 2.2) show mean levels ( $0.27 \pm 0.05$  ppbw from December 26<sup>th</sup> to 27<sup>th</sup> and  $0.29 \pm 0.07$  ppbw from January 2<sup>nd</sup> to 4<sup>th</sup>) that are well below the maximum seen in the snow-pit profiles (0.8 ppbw at 8 cm depth for the December 27<sup>th</sup> pit and 1.0-1.2 ppb between 5 and 15 cm depth in the January 9<sup>th</sup> pit). Such a large variability in the HCHO mixing ratios in the uppermost snow layers was often reported in previous studies conducted at other polar sites. It has been suggested that this is due to the presence or absence of freshly deposited snow that is always more enriched in HCHO with respect to atmospheric mixing ratios than aged snow

1 layers (Hutterli et al., 1999, 2002, and 2004). Under Concordia conditions, as discussed in  
2 Sect. 4.3, snow in equilibrium with the atmosphere in summer would contain at least 2.6  
3 ppbw of HCHO.

4 In the January 9<sup>th</sup> snow-pit, the maximum of HCHO mixing ratios seen from 5 to 15 cm  
5 below the surface (Fig. 4b) coincides with two relative maxima of sodium suggesting that  
6 they correspond to winter snow layers. Given the typical snow accumulation of 10 cm of  
7 snow at Concordia these two depths correspond to winter 2011 and winter 2010. For the  
8 December 27<sup>th</sup> snow-pit, the wide maximum of HCHO still coincides with these two winter  
9 layers seen in the corresponding sodium profile. The HCHO profile obtained by Hutterli et al.  
10 (2002) is more flat with a less variable value between 5 and 25 cm below the surface. In the  
11 absence of sodium data in this previous study, it remains difficult to conclude whether that is  
12 due to a strong wind driven redistribution of summer and winter snow layers by the wind at  
13 the snow pit location sampled by Hutterli et al. (2002) in 1998.

14 HCHO snow-pit profiles are also available from South Pole (Hutterli et al., 2004) and  
15 Summit in central Greenland (Hutterli et al., 1999). At both sites, winter HCHO maxima  
16 close to ~4-6 ppbw were observed. Deeper in the snow at 1.6 m depth, concentrations  
17 decrease to a nearly constant level of 4 ppbw at Summit and 0.3-1.1 ppbw at South Pole. The  
18 higher concentration observed in deeper snow layers at Summit than at South Pole was  
19 suggested to be driven by the fact that the mean snow accumulation rate is higher at Summit  
20 ( $22 \text{ g H}_2\text{O cm}^{-2} \text{ yr}^{-1}$ ) than at South Pole ( $6\text{-}11 \text{ g H}_2\text{O cm}^{-2} \text{ yr}^{-1}$ ) (Hutterli et al., 2002). The  
21 larger snow accumulation at Summit permits a better preservation of the atmospheric signal  
22 that dominates the weaker uptake capacity of HCHO in snow and ice at warmer temperatures  
23 (Burkhart et al., 2002; Barret et al., 2011a) at Summit compared to South Pole (mean annual  
24 T of  $-31^\circ\text{C}$  instead of  $-49^\circ\text{C}$  at South Pole). Thus, considering the quite similar temperatures  
25 at Concordia and South Pole (mean annual T of  $-54^\circ\text{C}$  compared to  $-49^\circ\text{C}$  at South Pole), the  
26 lower mean snow accumulation ( $2.8 \text{ g H}_2\text{O cm}^{-2} \text{ yr}^{-1}$  compared to  $6\text{-}11 \text{ g H}_2\text{O cm}^{-2} \text{ yr}^{-1}$  at  
27 South Pole) may reduce the preservation there, explaining the lower content in deep snow  
28 layers at Concordia than at South Pole.

## 30 **4.2 HCHO in interstitial Air**

31 During both the 2011/12 and 2012/13 field campaigns, investigations were made to  
32 document HCHO in the interstitial firn air (Fig. 5). The mean value observed at 20 cm depth  
33 in 2012/13 ( $530 \pm 95 \text{ pptv}$ ) largely exceeds the one in the atmosphere ( $\sim 130 \text{ pptv}$  observed in  
34 2011/12 and  $135 - 170 \text{ pptv}$  observed in 2012/13). Similar enhancements of HCHO in firn air

have been seen in a previous study conducted at South Pole (750 pptv at 10 cm depth against 103 pptv in the atmosphere, Hutterli et al., 2004). Fig. 4 and 5 show that, similar to the HCHO profile in snow, firn air HCHO levels show highest values near the snow surface and decreasing levels with depth, reaching values lower than 100 pptv below 80 cm depth. Whereas the here presented data of the HCHO change with depth in firn air is unique for Antarctica (no depth profile of interstitial air content is available from South Pole) a similar depth profile has been reported for Summit by Hutterli et al. (1999), with 1500-2000 pptv at 5-20 cm below the snow surface (compared to 230 pptv in the atmosphere) and 400 pptv at 1.5 m below the surface. The elevated mixing ratios in the firn air at Concordia with respect to those in the atmosphere point out the snowpack as a source of HCHO for the atmosphere in summer.

As seen in Fig. 6, HCHO mixing ratios measured at -20 cm in firn air coincide more closely with the daily course of temperature measured above the surface and at -20 cm than with the daily course of irradiance peaking at noon. Thus, the temperature variation in the uppermost snow layers should drive the HCHO firn air mixing ratios there, which tend to increase at warmer temperatures. In addition, during the first week of January the daily mean HCHO mixing ratio at -20 cm (600 pptv) was higher than the one after January 9<sup>th</sup> (400 pptv) in relation with a decrease of the temperature from -27.5°C to -31.3°C. This dependence of HCHO firn air in the upper snow-pack will be discussed further in the next section.

## 4.3 The firn air-snow partitioning at Concordia

### 4.3.1. The HCHO-ice thermodynamic equilibrium

On the basis of laboratory experiments, two studies investigated the HCHO partitioning between air and ice. The first attempt was made by Burkhart et al. (2002) who conducted laboratory experiments with pure ice between -5° and -35°C. However, as emphasized by Burkhart et al. (2002), the duration of laboratory experiments (less than 2 days) was not long enough to permit the ice to reach equilibrium, in particular at -35°C. In a more recent study Barret et al. (2011a) measured the solubility and the diffusivity of HCHO in ice between -7 and -30°C showing that the partitioning of HCHO between snow and atmosphere can be described by  $K(T) = X_{\text{HCHO}} / (P_{\text{HCHO}})^{0.803}$  (with  $X_{\text{HCHO}}$  being the HCHO molar fraction,  $P_{\text{HCHO}}$  being in Pa and T in K), in which K(T) follows an Arrhenius law. This equilibrium law is reported in Fig. 7 (black solid line) along with the one (black dashed line) from Burkhart et al.

(2002), the large difference between the two derived laws at low temperatures clearly reveals the under-saturation of the ice in the experiments conducted by Burkhart et al. (2002).

A few studies attempted to compare the partitioning of HCHO between air and snow observed during field campaigns with the thermodynamic equilibrium obtained in laboratory studies. This was done by Burkhart et al. (2002) with bulk snow and firn air data obtained by Hutterli et al. (1999) in a 3 m snow-pit dug at Summit. Barret et al. (2011b) examined whether the Alaskan Arctic snowpack follows the thermodynamic equilibrium. However, it has to be emphasized that in this latter study, air concentrations were not measured in the snowpack and were assumed to be identical to those measured 60 cm above the surface snow (see discussions below). Even more limited were examinations of the HCHO partitioning between air and snow in Antarctica as firn air measurements are very rarely available there. Hutterli et al. (2004) performed a few firn air measurements at 10 cm below the surface at South Pole in December 2000. These previous data (Summit, Barrow, and South Pole) are reported in Fig. 7 together with those gained in this study at Concordia. Due to the existence of a residual diurnal temperature cycle at 20 cm below the surface (see Fig. 6), data from this depth were reported in Fig. 7 as 10 min means, while those from further down were averaged over each of the 6 periods assigned in Fig. 2. The  $X_{\text{HCHO}}$  values used in calculations of  $K(T)$  reported in Fig. 7 were derived from the mean snow-pit profile reported in Fig. 4.

As seen in Fig. 7, all data from Concordia indicate under-saturation of snow by a factor of 10 with respect to interstitial air. We notice that, whereas no significant difference appears between the two sets of data derived using firn air values collected in 2011/12 and 2012/13, data corresponding to -70 cm in the 2012/13 experiment show systematically lower  $K(T)$  values. This latter difference is caused by the relatively high firn air mixing ratios seen at 70 cm depth in 2012/13 when compared to observations made just above and below (see Fig. 5). Thus we can not exclude that the firn air sampling at this depth might have been somewhat over-estimated as it might happen due to the presence of an inhomogeneous structure of the snow pack (i.e. depth hoar and/or wind crusts) what might have brought air from above to the inlet.

At the first glance, Fig. 7 suggests that the strong under-saturation of snow at Concordia is very unique compared to the other sites. However, as already mentioned, the Barrow data that considered atmospheric (and not firn air) mixing ratios certainly have led to a significant underestimation of the degree of under-saturation of snow. Furthermore, the single point reported for South Pole in Fig. 7 is calculated with 3.2 ppbw of bulk snow HCHO and a firn air value of 750 pptv (Hutterli et al., 2004), which is however probably diluted by

1 atmospheric air (Hutterli et al., 2004) leading to an underestimation of the degree of under-  
2 saturation of snow. Finally, at Summit, where snow and firn air profiles are well documented  
3 down to 2.5 m depth, a super-saturation was found at the surface followed by striking under-  
4 saturation 5 cm below the surface. Further down, at the depth of the preceding winter, an  
5 almost perfect thermodynamic equilibrium was observed. Then, except in the layer  
6 corresponding to the previous summer where snow is again under-saturated, most of the snow  
7 down to 2.5 m was close to the equilibrium. In conclusion, apart from Summit (with the  
8 noticeable exception of the snow located just below the surface), the polar snow appears often  
9 under-saturated with a particularly large depletion at Concordia. Note that, since a net HCHO  
10 flux out of the snow is detected during day and night at Concordia, the here calculated under  
11 saturation needs to be considered even as an upper value.

12       It is out of the scope of the present paper to investigate in detail the observed under-  
13 saturation of snow. At this stage we only assume (similarly as Hutterli et al., 1999) that there  
14 is a process acting in summer, leading to a strong under saturation of firn with respect to the  
15 thermodynamic air-ice equilibrium. This under saturation is counteracted by (1) precipitation,  
16 fog and frost events which add super saturated snow to the existing snowpack (Hutterli et al.,  
17 2004, Jacobi et al., 2002, Barret et al., 2011b), and (2) HCHO rich snow layers further down  
18 originating from the preceding winter season (Hutterli et al., 1999, 2003). If the snow  
19 accumulation is, however extremely low as at in Dome C, the preceding winter layer is still  
20 near the surface in summer, and super saturated fresh snow is added only seldomly to the  
21 snowpack. As a result, the regime of extreme under saturation acts probably throughout the  
22 entire snowpack, confirmed by our measurements, at least in snow layers down to 1 m  
23 corresponding to ages of the last ~10 year. However designing a more sophisticated modeling  
24 approach would require further data from Concordia obtained during winter in view to gain  
25 year-round information of HCHO in atmospheric air as well as in the interstitial air in the  
26 upper centimeters of the snow-pack.

27       As already shown by Fig. 6, Fig. 7 suggests a temperature driven dependence of the firn  
28 air-snow partitioning at Concordia. The slope of the linear regression obtained with data at -  
29 20 cm in the Arrhenius law in Fig. 7 (2.18 with  $R^2 = 0.5$ ), for which a large range of  
30 temperature is encountered, is quite similar (only 20% higher) than the one of the  
31 thermodynamic equilibrium calculated by Barret et al. (2011a).

### 4.3.2. Possible photochemical HCHO production in the snow-pack

As discussed in the preceding section, the assumption that snow emissions are controlled by temperature-driven exchanges (Hutterli et al., 2003) seems to be confirmed for Concordia conditions. While different experiments conducted at Alert and Barrow (Canadian and Alaskan Arctic) showed that HCHO emissions due to photolytic degradation of organic matter are present there (Barret et al., 2011b and references therein), this photolytic HCHO production seems to be very limited at inland polar ice sheet sites such as Summit (Hutterli et al., 1999) and South Pole (e.g. < 20% at South Pole) (Hutterli et al., 2004). To check directly whether the conclusion drawn for South Pole remains correct for Concordia, shading experiments were performed in January 2012 (see Sect. 2.2). No impact of cutting incident UV-radiation (wavelengths < 380 nm) on HCHO firn air concentrations at 10 cm below the surface snow depth was detected. This absence of changes does however not mean that no photochemical degradation of organic matter takes place, since the photolytic degradation of HCHO is also reduced during shading. Assuming a mean e-folding depth of 15 cm between 350 and 450 nm as measured by France et al. (2011) at Concordia in summer, and considering the HCHO photolytic rate during the shading experiment ( $J_{\text{HCHO-rad}} + J_{\text{HCHO-mol}}$  of  $1.7 \cdot 10^{-4} \text{ s}^{-1}$  at 14:00 LT for instance) we calculate that the photochemical production from organic matter, that may have been compensated by the photolytic HCHO destruction, would not contribute more than 15% of the HCHO mixing ratio at 10 cm depth (500-600 pptv during this experiment). Such a weak impact of the degradation of organic matter in HCHO at Concordia is not surprising considering the difference in recent values of dissolved organic carbon (DOC) measured at Concordia and Barrow. Indeed, while Legrand et al. (2013) reported a mean value of 20 ppbC (parts per billion of carbon) in the upper 10 cm surface snow at Concordia, Dominé et al. (2011) reported for snow and diamond dust layers at Barrow DOC levels ranging between 100 and 400 ppbC.

## 5. Estimates of HCHO snow emissions at Concordia

### 5.1. Estimation derived from vertical gradient of atmospheric concentrations

HCHO snow emission fluxes (F-HCHO) were derived from mixing ratios measured at 1 cm and 1 m above the snow surface using the integrated flux gradient method (e.g. Lenschow, 1995) detailed by Frey et al. (this issue). In brief, the turbulent flux F-HCHO in the surface layer is parameterized according to the Monin-Obukhov similarity theory (MOST). For each 30 min, a mean HCHO gradient was calculated from the 15 min averaged mixing ratios successively observed at 1 m and 1 cm.



As discussed in Frey et al. (this issue), MOST requires that mixing ratios at 1 m and 1 cm are significantly different. Therefore, 30 min vertical gradients that were smaller than their respective  $1 \sigma$  standard error, determined by error propagation of the  $1 \sigma$  standard variability of HCHO mixing ratios, were not included in the calculations. In this way, from December 14<sup>th</sup> to 18<sup>th</sup>, 77 values of a total of 114 were considered, and 152 of 200 from December 18<sup>th</sup> to 29<sup>th</sup>, respectively. Note however that 90% of the considered values of the vertical gradient stay below the mean detection limit of  $(27 \pm 9 \text{ pptv})$  calculated for the December 14<sup>th</sup> to December 28<sup>th</sup> period (see Fig. 1b). In addition, the application of the MOST theory also requires that the upper inlet height (1 m) is situated in the surface layer, i.e. below a height corresponding to 10% of the PBL height. If applied, this condition eliminates most of the nighttime data since the simulated PBL height are as low as 10 m or less in 80% of cases between 21:00 LT and 5:00 LT over the December 14<sup>th</sup> to 28<sup>th</sup> period. Though these data are more uncertain than the others, in Fig. 3 we report fluxes calculated between 21:00 LT and 5:00 LT (grey area) anyway, even when this second condition for the applicability of the MOST model is not reached. As seen in Fig. 3 the arithmetic mean and median HCHO snow emission fluxes remain in fairly good agreement reflecting the absence of 30 min data outliers.

Daily average F-HCHO values of  $-0.36 \pm 1.6 \times 10^{12} \text{ molecules m}^{-2} \text{ s}^{-1}$  and of  $2.7 \pm 2.7 \times 10^{12} \text{ molecules m}^{-2} \text{ s}^{-1}$  were calculated for the period between December 14<sup>th</sup> to 18<sup>th</sup> and December 19<sup>th</sup> to 28<sup>th</sup>, respectively. Being quasi-null over the first period, the calculated snow flux becomes positive from December 19<sup>th</sup> and 28<sup>th</sup>. Whereas no systematic change over the course of the day can be detected during the first period, a maximum during the day ( $\sim 4 \times 10^{12} \text{ molecules m}^{-2} \text{ s}^{-1}$  from 8:00 LT to 17:00 LT against  $1 \times 10^{12} \text{ molecules m}^{-2} \text{ s}^{-1}$  from 20:00 LT and 4:00 LT) was noticeable during the second half of December. Note that this increase of F-HCHO during the day results not only from the observed enhancement of the vertical gradient between 1 cm and 1 m (16 pptv from 8:00 LT to 17:00 LT against -6 pptv from 20:00 LT and 4:00 LT) but also from the increase of the friction velocity at that time of the day (Gallée et al., this issue). Both the increase of daily mean F-HCHO values from prior to after December 18<sup>th</sup> and the appearance of a diurnal maximum after December 19<sup>th</sup> are consistent with an increase of the snow air flux with enhanced temperatures as discussed in Sect. 4.3.1.

## 5.2. Estimations derived from interstitial firn air measurements

1 In view of the limited time period of available measurements and of the high  
2 uncertainty of the HCHO snow flux values derived from the relatively weak vertical HCHO  
3 gradients between 1 cm and 1 m (see Sect. 5.1) we try to estimate HCHO snow fluxes also on  
4 the base of HCHO gradients observed between the interstitial air and the atmosphere. One  
5 advantage of this approach lies in the fact that the transport of HCHO in firn air is slower than  
6 the one in the free atmosphere leading to firn-atmosphere gradients that would largely exceed  
7 the detection limit of HCHO measurements.

8 In order to estimate firn air-atmosphere snow fluxes, Fick's Law can be applied using  
9 measured concentration gradients between firn air and the atmosphere and the effective  
10 diffusion coefficient ( $D_{\text{eff}}$ ) in the open pore space. Since the turbulent diffusion in air above  
11 the snow is much larger than the diffusivity in firn air, the main concentration gradient will be  
12 in firn. Since HCHO air measurements made in 2011/2012 (see Fig. 3) indicate a vertical  
13 gradient of only a few pptv it is legitimated to use mixing ratios on the MT inlet at ~2 m as  
14 representative of HCHO level just above the surface.

15 Vertical transport in firn air of the top centimeters of the snowpack will depend on the  
16 molecular diffusion but can be significantly increased at high wind speed due to forced  
17 ventilation (Albert, 2002). Following Schwander et al. (1989) an effective molecular diffusion  
18 in firn ( $D_{\text{eff}}$ ) close to  $1.3 \times 10^{-5} \text{ m}^2 \text{ s}^{-1}$  is calculated for conditions at Concordia (at 650 mbar,  
19 244 K and a snow density of  $0.35 \text{ g cm}^{-3}$ ). Previous studies dealing with firn air-atmosphere  
20 gradients in Antarctica (Hutterli et al., 2004; Frey et al., 2005) assumed that with wind speed  
21 lower than  $5 \text{ m s}^{-1}$ , the wind pumping should have no significant influence with respect to  
22 molecular diffusion on motion in firn. However, more recently Seok et al. (2009) found a  
23 anti-correlation between wind speed and  $\text{CO}_2$  firn air gradients in the winter snowpack at a  
24 subalpine site in Colorado even at low wind speeds (a decrease by 50% of the gradient when  
25 wind speed increases from 0 to  $3 \text{ m s}^{-1}$ ). Therefore, we examine the dependence of the HCHO  
26 gradients between -20 cm and the atmosphere at Concordia with air temperature and wind  
27 speed data. The multi regression of HCHO gradients ( $R^2 = 0.5$ ) suggests a ~50 pptv decrease  
28 of the HCHO gradient when the wind speed reaches  $5 \text{ m s}^{-1}$ , what can make up to ~10 % of  
29 HCHO gradients during certain time periods. Therefore, this effect of forced ventilation was  
30 considered in the HCHO flux reported below.

31 The approach used here to estimate the fluxes assumes a constant diffusivity coefficient  
32 and thus a linear change of mixing ratios between the two measurement levels. As discussed  
33 in Sect. 4, HCHO firn air levels are expected to reach a maximum in the uppermost 10 cm of  
34 the snowpack and therefore the use of firn air data at -20 cm would significantly

underestimate the calculated HCHO fluxes. Therefore, an attempt was made to estimate HCHO mixing ratios in firn air near the surface by using the overall observed partitioning between snow and firn air observed at -20 cm below the surface (Fig. 7) as a function of temperature, and the mean snow pit content measured between 4 and 10 cm (means of 0.80 and 0.94 ppb). The daily course of the firn temperature at 7 cm below the surface was taken as the mean of air and snow (at 20 cm below the surface) temperatures.

Fig. 6 shows results obtained over two periods of the 2012/13 experiment, during which different mean air temperatures were encountered. It can be seen that HCHO levels at -7 cm are clearly enhanced (up to 240 pptv) compared to HCHO levels measured at -20 cm during the day, but are similar to the latter ones at night. Following calculations described above, mean HCHO fluxes out of the snow of  $2.6 \pm 0.8 \times 10^{12}$  molecule  $\text{m}^{-2} \text{s}^{-1}$  and  $1.8 \pm 0.7 \times 10^{12}$  molecule  $\text{m}^{-2} \text{s}^{-1}$  are calculated for the two periods during which mean air temperatures of -27.4 °C and -31.3 °C prevailed, respectively. Note that a significantly lower value ( $0.65 \times 10^{12}$  molecule  $\text{m}^{-2} \text{s}^{-1}$ ) is calculated for the end of January when mean air temperatures dropped to -37.5°C.

Applying this approach to the December 2011 campaign over the periods of December 14<sup>th</sup> to 18<sup>th</sup> (mean air temperature of -35°C) and December 19<sup>th</sup> to 28<sup>th</sup> (mean air temperature of -29°C) HCHO fluxes of  $0.85 \pm 0.36 \times 10^{12}$  molecule  $\text{m}^{-2} \text{s}^{-1}$  and  $2.15 \pm 0.93 \times 10^{12}$  molecule  $\text{m}^{-2} \text{s}^{-1}$  are estimated, what is (given the uncertainties of  $\pm 3$  cm in snow depth and of 0.08 ppbw in bulk snow HCHO) in good agreement with the corresponding flux estimates ( $-0.36 \pm 1.6 \times 10^{12}$  molecule  $\text{m}^{-2} \text{s}^{-1}$  from December 14<sup>th</sup> to 18<sup>th</sup> and  $2.7 \pm 2.7 \times 10^{12}$  molecule  $\text{m}^{-2} \text{s}^{-1}$  from December 19<sup>th</sup> to 28<sup>th</sup>) made in Sect. 5.1 on the base of atmospheric vertical gradients.

From the bulk snow content and an empirical partitioning between firn and in the snowpack, Hutterli et al. (2002) estimated a summer HCHO snow flux of  $\sim 0.2 \times 10^{12}$  molecule  $\text{m}^{-2} \text{s}^{-1}$  at Concordia, thus 10 times lower than is derived from atmospheric and firn air measurements made in our study. Since calculations of Hutterli et al. (2002) are based on a thermodynamic equilibrium, it is very likely that a large part of the difference comes from the large under-saturation of snow with respect to interstitial air as observed at Concordia (Sect. 4.3.1).

## 6. Sources and Sinks controlling the atmospheric budget of HCHO at Concordia

### 6. Reconstruction of the atmospheric summer HCHO budget at Concordia??

The importance of local gas phase photochemical productions and snow emissions on the atmospheric HCHO mixing ratios observed at 1 m above the snow surface at Concordia in summer were investigated with 1D model simulations. We performed calculations only for days with clear sky conditions (see Sect. 2.4). Whereas NO measurements started end of November 2011, those of OH and RO<sub>2</sub> are only available after December 19<sup>th</sup> and we focus therefore on the period from December 19<sup>th</sup> to 28<sup>th</sup>. The model was run each hour to simulate the daily cycle of HCHO mixing ratios. OH, HO<sub>2</sub> (estimated from RO<sub>2</sub> measurements, Kukui et al., 2014), NO, photolytic rates (see Sect. 2.2) and snow emission rates (see Sect. 5) were constrained by measurements. Their mean diurnal cycles are summarized in Fig. 8 together with the one of measured MHP. A CH<sub>4</sub> mixing ratio of 1758 ppbv was used as recorded in December 2011 at the Syowa Antarctic station (69°S). The HCHO snow emission fluxes considered in the model (hereafter denoted net HCHO snow flux) were calculated as the average of F-HCHO values derived from atmospheric HCHO gradients (Sect. 5.1) and of those derived from firn air-atmosphere gradients (Sect. 5.2).

## 6.1 Gas-phase photochemical sources and sinks of HCHO

In a first step simulations of the gas phase photochemistry only consider the CH<sub>4</sub> oxidation by OH together with the two major sinks of HCHO, namely the photolysis (reactions 11 and 12, Table 1) and the OH reaction (reaction 9, Table 1). Hereby the initial OH attack leads to the formation of the methyl peroxy (CH<sub>3</sub>O<sub>2</sub>) radical which can react with NO to form CH<sub>3</sub>O, which is then rapidly converted to HCHO with O<sub>2</sub> (reactions 1 to 3, Table 1). This reaction sequence is the dominant pathway under high NO conditions as encountered at Concordia whereas at low NO levels it would compete with reactions 4 to 6 (Table 1). Simulations indicate that this methane oxidation pathway leads to steady-state mixing ratios of 56 pptv and 91 pptv at noon and midnight, respectively (Fig. 9a).

MHP can form HCHO, CH<sub>3</sub>O or CH<sub>3</sub>O<sub>2</sub> (reactions 7, 8, and 10, Table 1). Since MHP measurements are available, the MHP contribution to the production of HCHO was examined separately from the CH<sub>4</sub> oxidation pathway with OH and NO (reactions 1 to 6, 9, 11, and 12, Table 1). As seen in Fig. 8, a daily mean MHP mixing ratio of ~50 pptv was observed at Concordia, which is nearly one half of the one reported by Frey et al. (2005) for South Pole. On the other hand, our model simulates a MHP mixing ratio of 20 pptv, suggesting that the MHP budget at Concordia is at least to ~40 % made up by CH<sub>4</sub> oxidation. Using observed MHP mixing ratios we calculate that ~ 15 pptv of HCHO are linked to the MHP breakdown (Fig. 9). Thus the MHP pathway accounts for 17% of the total HCHO production originating

from the CH<sub>4</sub> oxidation at Concordia. That is virtually the same what was obtained at DDU (Preunkert et al., 2013), but only half of the corresponding value (i.e. 36 %) observed in the marine boundary layer (Wagner et al., 2002). As already concluded by Preunkert et al. (2013), this is due to the high level of NO, which strengthens the OH/NO methane oxidation pathway (reaction 2) with respect to the HO<sub>2</sub> and MHP pathway (reaction 6).

On the basis of DOAS measurements made at Concordia, Frey et al. (this issue) estimated that 2 to 3 pptv of BrO are present near the surface. Assuming a daily mean value of 2.5 pptv of BrO we estimated the Br level to be of 0.43 pptv from steady state calculations considering the BrO photolysis and the Br reaction with O<sub>3</sub>. Using these values and considering reactions 13-15 of Table 1, we found that the Br chemistry represents a net HCHO loss that remains limited to -3 pptv to -10 pptv from noon to midnight (Fig. 9b).

As seen in Figure 8a the simulated HCHO daily cycle resulting from the overall gas phase chemistry accounts for 70 pptv and 95 pptv (i.e. 65 % and 68 % of the observed HCHO level) at noon and at midnight, respectively. Such a large contribution of the local gas phase chemistry was also found for South Pole, where oxidants are of similar abundance than at Concordia. Thus with  $2 \times 10^6$  molecules cm<sup>-3</sup> of OH and 88 pptv of NO (Eisele et al., 2008) consistently to Concordia ~70 % of the observed 110 pptv of HCHO were explained by the gas phase chemistry (Hutterli et al., 2004) at South Pole.

## **6.2 The impact of snow emissions on the HCHO budget**

As mentioned in Sect. 3 (see also Fig. 9a) the diurnal HCHO cycle observed over the period from 19<sup>th</sup> to 28<sup>th</sup> December 2011 is characterized by a daytime minimum with amplitude reaching 30 pptv. The simulated diurnal cycle related to the gas phase chemistry reproduces a similar diurnal cycle but with a slightly weaker amplitude (~ 30 pptv), and simulated HCHO mixing ratios underestimate observations by ~40 pptv at noon and ~55 pptv at night.

Considering the net HCHO snow flux (see Fig. 8) in addition to the above discussed gas phase chemistry, a daily mean HCHO mixing ratio of 112 pptv is calculated, slightly lower compared to the observed 128 pptv. While simulations are in good agreement from 20:00 LT to 4:00 LT (Fig. 9a) they tend to underestimate observations by  $30 \pm 9$  pptv from 9:00 LT to 15 LT. The simulated values indicate that HCHO snow emissions account for ~ 30 % of the observed HCHO mixing ratio at night and around 10 % at noon.

Note that, since the values of the HCHO snow emission rates are based on in situ measurements, they represent the net HCHO flux that includes also the effect of dry deposition. Therefore no dry deposition was considered in the simulations.

### 6.3. Uncertainties of model calculations

Simulations of (gas-phase chemistry plus snow emissions) indicate a better agreement with observations during the night than during the day. We investigated to what extent the uncertainties of simulations depend on the time of day and which parameters are responsible for that. The uncertainties of the preceding calculations include those linked to the kinetic rates of gas phase calculations but are also related to the day to day variability of the hourly values used for OH, HO<sub>2</sub>, NO, MHP, photolysis rates and the uncertainty of the net HCHO snow emission flux as reported in Fig. 8. The uncertainty of the simulated turbulent transport needs also to be examined.

To evaluate the uncertainty linked to the kinetic rates of the main gas phase HCHO production processes, a Monte-Carlo study was performed in which all of the rate constants involved in methane oxidation (reactions 1 to 9, Table 1) were modified simultaneously and independently of each other accordingly to their probability distribution (see Preunkert et al. (2013) and Wagner et al. (2002) for further details). Including 1000 model runs the uncertainty ( $\pm 1 \sigma$ ) of calculations related to the kinetic rates is close to  $\pm 10$  pptv (i.e. 10% of calculated values) under daily mean Concordia summer conditions.

A Monte-Carlo study was also applied to evaluate uncertainties resulting from the daily variability of OH, HO<sub>2</sub>, NO, MHP, photolysis rates, and the calculated uncertainty of the HCHO net snow emission. The overall HCHO error derived from this Monte-Carlo study reaches  $\pm 13$  pptv from 8:00 LT to 18:00 LT (mean simulated value of 88 pptv) and  $\pm 26$  pptv from 20:00 LT to 4:00 LT (mean simulated value of 140 pptv). Although the 10% uncertainty of the CH<sub>4</sub> oxidation constant rates are not included in errors reported in Fig. 9a, it can be seen that HCHO simulated values match observations during the night but underestimate them slightly during the day.

Fig. 9c indicates the relative contribution of each parameter to the total uncertainty. It can be seen that during the day (from 8:00 LT to 18:00 LT) the main uncertainty is related to the variability of OH, the uncertainty of the net HCHO snow flux, and the strong daily variability of MHP, accounting for 33%, 31%, and 19%, respectively. During the night (from 20:00 LT to 4:00 LT), 57% of the uncertainty is related to the net snow flux uncertainties and 20% from the variability of OH. Note that the variability of NO plays no significant role on

1 the uncertainty of simulated HCHO values, likely due to the excess of NO prevailing at  
2 Concordia which ensures minor influence of peroxy radicals self reactions compared to the  
3 reaction with NO (reaction 2, 4 and 5, Table 1).

4 Finally, the influence of the strength and the height of the simulated turbulent transport  
5 was tested by increasing and decreasing Kz values and the height of the vertical model levels  
6 by 30%, variations as typically encountered with MAR simulations for Kz values and the  
7 estimated PBL height even under clear sky conditions (Gallée et al., this issue). In brief, a  
8 successive decrease of Kz values and vertical level heights by a factor of 0.7 increases  
9 calculated HCHO mixing ratios by  $\sim 10$  and  $20$  pptv at midnight, respectively, while at noon  
10 the increase is limited to  $\sim 3$  and  $6$  pptv, respectively. Similarly, a successive increase of Kz  
11 values and vertical level heights by a factor of 1.3 decreases calculated HCHO mixing ratios  
12 by  $\sim 7$  and  $12$  pptv at midnight, respectively, while at noon the decrease is only  $\sim 2$  and  $1.5$   
13 pptv, respectively. As for uncertainties related to HCHO net snow emission fluxes (Fig. 9c),  
14 higher uncertainty are encountered during the night due to the very low Kz values and a very  
15 shallow mixing height prevailing at Concordia at that time, making atmospheric HCHO  
16 mixing ratios sensitive to any change of the snow emissions and of the vertical transport. As a  
17 result, even when only clear sky conditions were considered in the calculations, uncertainties  
18 in the strength and the height of the simulated turbulent transport might at least increase the  
19 uncertainties of our HCHO calculations by 10 to 15 %.

21 When considering all above discussed uncertainties, atmospheric HCHO mixing ratios  
22 of  $89 \pm 22$  pptv for 8:00 LT to 18:00 LT and  $140 \pm 40$  pptv for 20:00 LT to 4:00 LT are  
23 calculated. These values are consistent with observations (i.e.  $116 \pm 16$  pptv from 8:00 LT to  
24 18:00 LT and  $140 \pm 10$  pptv 20:00 LT to 4:00 LT), suggesting that no relevant HCHO source  
25 or sink has been missed in our estimation.

26 Previous 1-D HCHO simulations were made assuming that near-surface observed levels  
27 of NO and HO<sub>x</sub> are constant within the whole PBL. Given the photochemical lifetime of  
28 HCHO (close to 1 h at noon and 7 h at night), we may expect a rather homogeneous  
29 distribution of HCHO within the PBL and the simulated HCHO value at 1 m would depend  
30 on the total production acting within the PBL. Therefore, the calculated HCHO value at 1 m  
31 depends on the vertical gradient of HO<sub>x</sub> and NO. As detailed by Frey et al. (this issue), a few  
32 vertical profiles of NO were obtained during balloon flights up to 100 m. It appears that  
33 during daytime the lower PBL is well mixed with quasi unchanged NO mixing ratios between  
34 2.5 and 100 m. Concerning OH and HO<sub>2</sub> for which no data are available above 3 m, we may

expect only little change with height, since the unchanged levels of NO make unchanged the main source of OH, namely the recycling of RO<sub>2</sub> by NO that represents here more than a half of the total OH production at noon (Kukui et al., 2014). The second half of the total OH production corresponds to primary productions from ozone and H<sub>2</sub>O<sub>2</sub> (representing together 50%) and HONO (50%, considering the bias in measurements of this species discussed in Legrand et al., 2014) (Kukui et al., 2014). Ozone vertical profiles were regularly done during the OPAL campaign showing well-mixed levels within the lower 100 m during day and night. Given the atmospheric lifetime of H<sub>2</sub>O<sub>2</sub> (9 h against photolysis at noon), we can expect an absence of vertical gradient for this species as well. In fact, only for HONO a strong vertical gradient is expected given the suspected importance a surface snow source and a lifetime of 5 min at noon (Legrand et al., 2014). Therefore, assuming an overestimation of HONO by a factor of 4 as discussed in Kukui et al. (2014), a limited vertical change of HO<sub>x</sub> within the PBL is expected, and consequently the assumption of a similar HCHO photochemical production throughout the whole PBL is reasonable. Reversely, the consistency between HCHO observations and simulations made considering constant HO<sub>x</sub> levels within the PBL tends to support the conclusion of an overestimation of HONO measurements, as drawn independently by Legrand et al. (2014) and Kukui et al. (2014).

## 7. Summary

This first study of ambient air HCHO measurements at Concordia indicates typical summer mixing ratios of 130 pptv. Model simulations indicate that the net gas-phase production from methane oxidation accounts largely (66%) to observed mixing ratios in relation with the observed high levels of OH and NO there in summer. HCHO measurements conducted in the three environmental compartments (ambient air, firn air, and snow) confirm that the snow at Concordia is a net source of HCHO in summer throughout day and night. Though a strong under-saturation of the snow-pack with respect to interstitial air compared to the pure ice-air thermodynamic equilibrium is observed, no significant change in HCHO production was observed during shading experiments suggesting that snow emissions are mainly controlled by temperature-driven exchanges rather than by photolytic degradation of organic matter. Snow emission fluxes estimated from vertical gradients between 1 cm and 1 m above the snow surface and between air just below and above the snow surface consistently suggest levels between 1 and 2 x 10<sup>12</sup> molecules m<sup>-2</sup> s<sup>-1</sup> at night and 3 to 5 x 10<sup>12</sup> molecules m<sup>-2</sup> s<sup>-1</sup> at noon. 1-D simulations considering these snow emissions and the gas phase chemistry (mainly the methane oxidation) calculate a daily mean HCHO mixing ratio of 112 pptv, in



1 good agreement with the observed  $\sim 130$  pptv, show however an underestimate by 30 pptv at  
2 mid-day. Further field works with particular emphasize on measurements in the 3  
3 compartments in winter are mandatory to better understand the overall strong under-saturation  
4 of snow at that site.  
5

## **Acknowledgements**

The OPALE project was funded by the ANR (Agence National de Recherche) contract ANR-09-BLAN-0226. National financial support and field logistic supplies for the summer campaign were provided by the Institut Polaire Français-Paul Emile Victor (IPEV) within programs N° 414, 903, and 1011. The 2012-2014 snowpack air sampling experiments were funded by an award to D. Helmig and J. Savarino from the United States National Science Foundation Office of Polar Programs (NSF #1142145). M.D. King was supported by NERC NE/F0004796/1 and NE/F010788, NERC FSF grants 555.0608 and 584.0609. We thank PNRA for providing temperature and pressure data at Concordia. Thanks to Edward J. Dlugokencky and the World data Center for Greenhouse Gases for providing CH<sub>4</sub> data from the Syowa station.

## References

- Albert, M. R., and Shultz, E. F.: Snow and firn properties and air- snow transport processes at Summit, Greenland, *Atmos. Environ.*, 36, 2789–2797, doi:10.1016/S1352-2310(02)00119-X, 2002.
- Atkinson, R., Baulch, D.L., Cox, R.A., Crowley, J.N., Hampson, R.F., Hynes, R.G., Jenkin, M.E., Rossi, M.J., Troe, J., and IUPAC Subcommittee: Evaluated kinetic and photochemical data for atmospheric chemistry: Volume II – gas phase reactions of organic species, *Atmos. Chem. Phys.*, 6(11), 3625-4055, doi:10.5194/acp-6-3625-2006, 2006.
- Atkinson, R., Baulch, D.L., Cox, R.A., Crowley, J.N., Hampson, R.F., Hynes, R.G., Jenkin, M.E., Rossi, M.J., and Troe, J.: Evaluated kinetic and photochemical data for atmospheric chemistry: Volume III - gas phase reactions of inorganic halogens, *Atmos. Chem. Phys.*, 7(4), 981–1191, doi:10.5194/acp-7-981-2007, 2007.
- Atkinson, R., Baulch, D.L., Cox, R.A., Crowley, J.N., Hampson, R.F., Hynes, R.G., Jenkin, M.E., Rossi, M.J., Troe, J., and Wallington, T.J.: Evaluated kinetic and photochemical data for atmospheric chemistry: Volume IV - gas phase reactions of organic halogen species, *Atmos. Chem. Phys.*, 8(15), 4141-4496, doi:10.5194/acp-8-4141-2008, 2008.
- Barret, M., Houdier, S., and Domine, F.: Thermodynamics of the Formaldehyde-Water and Formaldehyde-Ice Systems for atmospheric implications, *J. Phys. Chem. A*, 115(3), 307-317, doi:10.1021/jp108907u, 2011a.
- Barret, M., Domine, F., Houdier, S., Gallet, J.-C., Weibring, P., Walega, J., Fried, A., and Richter, D.: Formaldehyde in the Alaskan Arctic snowpack: Partitioning and physical processes involved in air-snow exchanges, *J. Geophys. Res.*, 116, D00R03, doi:10.1029/2011JD016038, 2011b.
- Beyersdorf A.J., D. R. Blake, A. Swanson, S. Meinardi, F.S. Rowland, and D. Davis: Abundances and variability of tropospheric volatile organic compounds at the South Pole and other Antarctic locations, *Atmos. Environ.*, 44(36), 4565-4574, doi:10.1016/j.atmosenv.2010.08.025, 2010.
- Bloss, W. J., J.D. Lee, D.E. Heard, R.A. Salmon, S. J.-B. Bauguutte, H.K. Roscoe, and A.E. Jones (2007), Observations of OH and HO<sub>2</sub> radicals in coastal Antarctica, *Atmos. Chem. Phys.*, 7(16), 4171-4185, doi:10.5194/acp-7-4171-2007.

- 1 Burkhardt, J.F., Hutterli, M.A., and Bales, R.C.: Partitioning of formaldehyde between air and  
2 ice at -35°C to -5°C, *Atmos. Environ.*, 36(13), 2157-2163, 2002.
- 3 Chen, G. et al.: A reassessment of HOx South Pole chemistry based on observations recorded  
4 during ISCAT 2000, *Atmos. Environ.*, 38(32), 5451-5461,  
5 doi:10.1016/j.atmosenv.2003.07.018, 2004.
- 6 Dasgupta, P. K., Dong, S., Hwang, H., Yang, H.-C., and Genfa, Z.: Continuous liquid-phase  
7 fluorometry coupled to a diffusion scrubber for the real-time determination of  
8 atmospheric formaldehyde, hydrogen peroxide and sulfur dioxide, *Atmos. Environ.*,  
9 22(5), 949-963, doi:10.1016/0004-6981(88)90273-9, 1988.
- 10 DeMore, W.B., Sander, S.P., Golden, D.M., Hampson, R.F., Kurylo, M.J., Howard, C.J.,  
11 Ravishankara, A.R., Kolb, C.E., and Molina, M.J.: Chemical kinetics and  
12 photochemical data for use in stratospheric modeling, Evaluation 12, JPL Publ., 97-4,  
13 JPL: Pasadena, CA, January 15, 1997.
- 14 Domine, F., Gallet, J.-C., Barret, M., Houdier, S., Voisin, D., Douglas, T.A., Blum, J.D.,  
15 Beine, H.J., Anastasio, C., and Bréon, F.-M.: The specific surface area and chemical  
16 composition of diamond dust near Barrow, Alaska, *J. Geophys. Res.*, 116, D00R06,  
17 doi:10.1029/2011JD016162, 2011.
- 18 Eisele, F., Davis, D. D., Helmig, D., Oltmans, S. J., Neff, W., Huey, G., Tanner, D., Chen, G.,  
19 Crawford, J., Arimoto, R., Buhr, M., Mauldin, L., Hutterli, M., Dibb, J., Blake, D.,  
20 Brooks, S. B., Johnson, B., Roberts, J. M., Wang, Y. H., Tan, D., and Flocke, F.:  
21 Antarctic Tropospheric Chemistry Investigation (ANTCI) 2003 overview, *Atmos.*  
22 *Environ.*, 42, 2749–2761, 2008.
- 23 France, J.L., King, M.D., Frey, M.M., Erbland, J., Picard, G., Preunkert, S., MacArthur, A.,  
24 and Savarino, J. : Snow optical properties at Dome C (Concordia), Antarctica;  
25 implications for snow emissions and snow chemistry of reactive nitrogen, *Atmos.*  
26 *Chem. Phys.*, 11, 9787–9801, 2011.
- 27 Frey, M.M., Steward, R.W., McConnell, J.R., and Bales, R.C.: Atmospheric hydroperoxides  
28 in West Antarctica: Links to stratospheric ozone atmospheric oxidation capacity, *J.*  
29 *Geophys. Res.*, 110, D23301, doi:10.1029/2005JD006110, 2005.
- 30 Frey, M.M., Brough, N., France, J.L., Anderson, P.S., Traulle, O., King, M.D., Jones, A.E.,  
31 Wolff, E.W., and Savarino, J.: The diurnal variability of atmospheric nitrogen oxides  
32 (NO and NO<sub>2</sub>) above the Antarctic Plateau driven by atmospheric stability and snow  
33 emissions, *Atmos. Chem. Phys.*, 13, 3045–3062, doi:10.5194/acp-13-3045-2013,  
34 2013.

- 1 Frey, M.M., Brough, N., Roscoe, H., Kukui, S., Savarino, J., Legrand, M., and Preunkert, S.:  
2 Drivers of atmospheric nitrogen oxide emissions from snow above the Antarctic  
3 Plateau in summer: sensitivity to stratospheric ozone and impact on ozone production,  
4 this issue.
- 5 Gallée, H. and Gorodetskaya, I.: Validation of a limited area model over Dome C, Antarctic  
6 29 Plateau, during winter, 34, 61 – 72, *Clim. Dyn.*, doi:10.1007/s00382-008-0499-  
7 y, 2008.
- 8 Gallée, H., S. Preunkert, S. Argentini, M. M. Frey, C. Genthon, B. Jourdain, I. Pietroni, G.  
9 Casasanta, H. Barral, E. Vignon, and M. Legrand, Characterization of the boundary  
10 layer at Dome C (East Antarctica) during the OPALE summer campaign, *Atmos.*  
11 *Chem. Phys.*, this issue.
- 12 Helmig, D., F. Bocqueta, L. Cohena, and S.J. Oltmans: Ozone uptake to the polar snowpack  
13 at Summit, Greenland, *Atmos. Environ.*, 41(24), 5061-5076, doi:  
14 10.1016/j.atmosenv.2006.06.064, 2007.
- 15 Hutterli, M.A., R. Rothlisberger, and R. C. Bales: Atmosphere-to-snow-to-firn transfer  
16 studies of HCHO at Summit, Greenland, *Geophys. Res. Lett.*, 26(12), 1691–1694,  
17 doi: 10.1029/1999GL900327, 1999.
- 18 Hutterli, M.A., Bales, R.C., McConnell, J.R., and Stewart, R.W.: HCHO in Antarctic snow:  
19 Preservation in ice cores and air-snow exchange, *Geophys. Res. Lett.*, 29(8), 1235,  
20 doi:10.1029/2001GL014256, 2002.
- 21 Hutterli, M. A., McConnell, J. R., Bales, R. C., and Stewart, R. W.: Sensitivity of hydrogen  
22 peroxide (H<sub>2</sub>O<sub>2</sub>) and formaldehyde (HCHO) preservation in snow to changing  
23 environmental conditions: Implications for ice core records, *J. Geophys. Res.*,  
24 108(4023), 10–1029.
- 25 Hutterli, M.A., McConnell, J.R., Chen, G., Bales, R.C., Davis, D.D., and Lenschow, D.H.:  
26 Formaldehyde and hydrogen peroxide in air, snow and interstitial air at South Pole,  
27 *Atmos. Environ.*, 38(32), 5439-5450, 2004.
- 28 Jacobi, H. W., Frey, M. M., Hutterli, M.A., Bales, R. C., Schrems, O., Cullen, N.J., Steffen,  
29 K., and Koehler, C.: Measurements of hydrogen peroxide and formaldehyde exchange  
30 between the atmosphere and surface snow at Summit, Greenland, *Atmos. Environ.*,  
31 36(15-16), 2619–2628, 2002.

- 1 Jun, L., Weili W. and Zwally, H.J.: Interannual variations of shallow firn temperature at  
2 Greenland summit, *Annals of Glaciology*, 35, 368-370, doi:  
3 <http://dx.doi.org/10.3189/172756402781816933>, 2002.
- 4 Kukui, A., Legrand, M., Ancellet, G., Gros, V., Bekki, S., Sarda-Estève, R., Loisil, R., and  
5 Preunkert, S.: Measurements of OH and RO<sub>2</sub> radicals at the coastal Antarctic site of  
6 Dumont d'Urville (East Antarctica) in summer, *J. Geophys. Res.*, VOL. 117, D12310,  
7 doi:10.1029/2012JD017614, 2012.
- 8 Kukui, A., Legrand, M., Preunkert, S., Frey, M., Loisil, R., Gil Roca, J., Jourdain, B., King,  
9 M., France, J., and Ancellet, G.: OH and RO<sub>2</sub> measurements at Dome C, East  
10 Antarctica, *Atmos. Chem. Phys.*, 12373–12392, doi:10.5194/acp-14-12373-2014,  
11 2014.
- 12 Legrand, M., Preunkert, S., Schock, M., Cerqueira, M., Kasper-Giebl, A., Afonso, J., Pio, C.,  
13 Gelencsér, A., and Dombrowski-Etchevers.: Major 20th century changes of  
14 carbonaceous aerosol components (EC, WinOC, DOC, HULIS, carboxylic acids, and  
15 cellulose) derived from Alpine ice cores, *J. Geophys. Res.*, 112, D23S11,  
16 doi:10.1029/2006JD008080, 2007.
- 17 Legrand, M., Preunkert, S., Jourdain, B., Guilhermet, J., Faïn, X., Alekhina, I., and Petit, J.R. :  
18 Water-soluble organic carbon in snow and ice deposited at Alpine, Greenland, and  
19 Antarctic sites: A critical review of available data and their atmospheric relevance,  
20 *Clim. Past*, 9, 2195-2211, doi:10.5194/cp-9-2195-2013, 2013.
- 21 Legrand, M., Preunkert, S., Frey, M., Bartels-Rausch, T., Kukui, A., King, M., Kerbrat, M.,  
22 Jourdain, B., and Savarino, J: High atmospheric levels of nitrous acid at Concordia  
23 (East Antarctic plateau) in summer: A strong source from surface snow ?, *Atmos.*  
24 *Chem. Phys.*, 14, 9963-9976, doi:10.5194/acp-14-9963-2014, 2014.
- 25 Lenschow, D. H.: Micrometeorological techniques for measuring biosphere-atmosphere trace  
26 gas exchange, in: *Biogenic Trace Gases: Measuring emissions from soil and water*,  
27 edited by Matson, P. A. and Harriss, R. C., pp. 126-163, Blackwell Science, London,  
28 1995.
- 29 Lowe, D. C., and Schmidt, U.: Formaldehyde (HCHO) measurements in the Nonurban  
30 Atmosphere, *J. Geophys. Res.*, 88(C15), 10,844-10,858,  
31 doi:10.1029/JC088iC15p10844, 1983.
- 32 Michalowski, B. A., J. S. Francisco, S.-M. Li, L. A. Barrie, J. W. Bottenheim, and P. B.  
33 Shepson, A computer model study of multiphase chemistry in the Arctic boundary  
34 layer during polar sunrise, *J. Geophys. Res.*, D12, 15131–15145, 105, 2000.

- 1 Preunkert, S., Jourdain, B., Legrand, M., Udisti, R., Becagli, S., and Cerri, O.: Seasonality of  
2 sulfur species (sulfate, methanesulfonate and dimethyl sulfur) in Antarctica: inland  
3 versus coastal regions, *J. Geophys. Res.*, 113, D15302, doi:10.1029/2008JD009937,  
4 2008.
- 5 Preunkert S., Ancellet, G., Legrand, M., Kukui, A., Kerbrat, M., Sarda-Estève, R., Gros, V.,  
6 and Jourdain, B.: Oxidant Production over Antarctic Land and its Export (OPALE)  
7 project: An overview of the 2010-2011 summer campaign, *J. Geophys. Res.*,  
8 doi:10.1029/2011JD017145, 2012.
- 9 Preunkert, S., Legrand, M., Pépy, G., Gallée, H., Jones, A., and Jourdain, B.: The atmospheric  
10 HCHO budget at Dumont d'Urville (East Antarctica): Contribution of photochemical  
11 gas-phase production versus snow emissions, *J. Geophys. Res. Atmos.*, 118, 13,319–  
12 13,337, doi:10.1002/2013JD019864, 2013.
- 13 Riedel, K., Weller, R., and Schrems, O.: Variability of formaldehyde in the Antarctic  
14 troposphere, *Phys. Chem. Chem. Phys.*, 1(24), 5523–5527, 1999.
- 15 Salmon, R. A., Bauguutte, S. J.-B., Bloss, W., Hutterli, M. A., Jones, A. E., Read, K., and  
16 Wolff, E. W.: Measurement and interpretation of gas phase formaldehyde  
17 concentrations obtained during the CHABLIS campaign in coastal Antarctica, *Atmos.*  
18 *Chem. Phys.*, 8(14), 4085-4093, doi:10.5194/acp-8-4085-2008, 2008.
- 19 Schwander, J., The transformation of snow to ice and the occlusion of gases, in *The*  
20 *Environmental Record in Glaciers and Ice Sheets*, edited by H. Oeschger, and C.C.  
21 Langway, Jr., pp. 53-67, John Wiley, New York, 1989.
- 22 Seok, B., Helmig, D., Williams, M.W., Liptzin, D., Chowanski, K., and Hueber, J.: An  
23 automated system for continuous measurements of trace gas fluxes through snow: an  
24 evaluation of the gas diffusion method at a subalpine forest site, Niwot Ridge,  
25 Colorado, *Biogeochemistry*, 95-95, 113, DOI 10.1007/s10533-009-9302-3, 2009.
- 26 Seinfeld, J.H., and Pandis, S.P., *Atmospheric Chemistry and Physics: From Air Pollution to*  
27 *Climate Change*, 2nd Edition, pp 1232, John Wiley, New Jersey, 2006.
- 28 Sumner, A. L., and Shepson, P. B.: Snowpack production of formaldehyde and its effect on  
29 the Arctic troposphere, *Nature*, 398, 230-233, doi:10.1038/18423, 1999.
- 30 Wagner, V., von Glasow, R., Fischer, H., and Crutzen, P.J.: Are CH<sub>2</sub>O measurements in the  
31 marine boundary layer suitable for testing the current understanding of CH<sub>4</sub>  
32 photooxidation?: A model study, *J. Geophys. Res.*, 107,  
33 doi:200210.1029/2001JD000722, 2002.

1 Yang J., Honrath, R. E., Peterson, M. C., Dibb, J. E., Sumner, A. L., Shepson, P. B., Frey, M.,  
2 Jacobi, H.-W., Swanson, A., and Blake, N.: Impacts of snowpack emissions on  
3 deduced levels of OH and peroxy radicals at Summit, Greenland, Atmos. Environ.,  
4 36(15-16), 2523-2534, 2002.

5



## Tables

**Table 1.** Gas-phase reactions included in the 1-D model (see Sect. 2.4). Kinetic rates are given in  $\text{cm}^3 \text{ molecule}^{-1} \text{ s}^{-1}$ . HCHO and MHP ( $\text{CH}_3\text{OOH}$ ) photolysis rates are reported in Fig. 8.

N°	Reactions	Kinetic rates	References
1	$\text{CH}_4 + \text{OH} + \text{O}_2 \rightarrow \text{CH}_3\text{O}_2 + \text{H}_2\text{O}$	$2.45 \times 10^{-12} \exp [-1775/T]$	a
2	$\text{CH}_3\text{O}_2 + \text{NO} \rightarrow \text{CH}_3\text{O} + \text{NO}_2$	$2.30 \times 10^{-12} \exp [360/T]$	b
3	$\text{CH}_3\text{O} + \text{O}_2 \rightarrow \text{HCHO} + \text{HO}_2$	$7.20 \times 10^{-14} \exp [-1080/T]$	b
4	$\text{CH}_3\text{O}_2 + \text{CH}_3\text{O}_2 \rightarrow 2 \text{CH}_3\text{O} + \text{O}_2$	$(7.40 \times 10^{-13} \exp [-520/T] - 1.03 \times 10^{-13} \exp [800/T]) 0.35$	b
5	$\text{CH}_3\text{O}_2 + \text{CH}_3\text{O}_2 \rightarrow \text{CH}_3\text{OH} + \text{HCHO} + \text{O}_2$	$(1.03 \times 10^{-13} \exp [800/T]) 0.65$	b
6	$\text{CH}_3\text{O}_2 + \text{HO}_2 \rightarrow \text{CH}_3\text{OOH} + \text{O}_2$	$3.80 \times 10^{-13} \exp [780/T]$	b
7	$\text{CH}_3\text{OOH} + \text{OH} \rightarrow \text{HCHO} + \text{HO} + \text{H}_2\text{O}$	$(2.93 \times 10^{-12} \exp [190/T]) 0.35$	b
8	$\text{CH}_3\text{OOH} + \text{OH} \rightarrow \text{CH}_3\text{O}_2 + \text{H}_2\text{O}$	$(1.78 \times 10^{-12} \exp [220/T]) 0.65$	b
9	$\text{HCHO} + \text{OH} \rightarrow \text{H}_2\text{O} + \text{HCO}$	$5.40 \times 10^{-12} \exp [135/T]$	b
10	$\text{CH}_3\text{OOH} \rightarrow \text{CH}_3\text{O} + \text{OH} (\lambda < 645\text{nm})$	$J_{\text{MHP}}$	
11	$\text{HCHO} \rightarrow \text{H}_2 + \text{CO} (\lambda < 337\text{nm})$	$J_{\text{HCHO-mol}}$	
12	$\text{HCHO} \rightarrow \text{H} + \text{HCO} (\lambda < 360\text{nm})$	$J_{\text{HCHO-rad}}$	
13	$\text{Br} + \text{HCHO} \rightarrow \text{HBr} + \text{HCO}$	$2.7 \times 10^{-12} \exp [-580/T]$	c
14	$\text{BrO} + \text{CH}_3\text{O}_2 \rightarrow \text{CH}_2\text{O}_2 + \text{HOBr}$	$5.70 \times 10^{-12}$	d
15	$\text{BrO} + \text{HCHO} \rightarrow \text{HOBr} + \text{HCO}$	$1.50 \times 10^{-14}$	e

<sup>a</sup>[DeMore *et al.*, 1997], <sup>b</sup>[Atkinson *et al.*, 2006], <sup>c</sup>[Atkinson *et al.*, 2007], <sup>d</sup>[Atkinson *et al.*, 2008], <sup>e</sup>[Michalowski *et al.*, 2000]

**Table 2.** Atmospheric HCHO mixing ratios in the lower Antarctic atmosphere.

Site	Date	HCHO (pptv)	Location	References
South Pole	Dec. 2000	103	89.98°S 24.8°W	Hutterli et al. (2004)
South Pole	2 - 4 Jan. 2003	155	89.91°S 147.57°W	Frey et al. (2005)
Byrd	28 Nov. 2011 - 11 Dec 2002	120 ± 50	80.02°S 119.6°W	Frey et al. (2005)
Halley	Dec. 2004 - Jan. 2005	90 - 140	75.58°S 26.65°W	Salmon et al. (2008)
DDU	Jan. 2009 and Dec. 2009	150 - 195	66.66°S 140.02E	Preunkert et al. ( 2013)
Concordia	14 Dec. 2011 – 11 Jan. 2012	130 ± 37	75.1°S 123.55°E	This study

# Figures

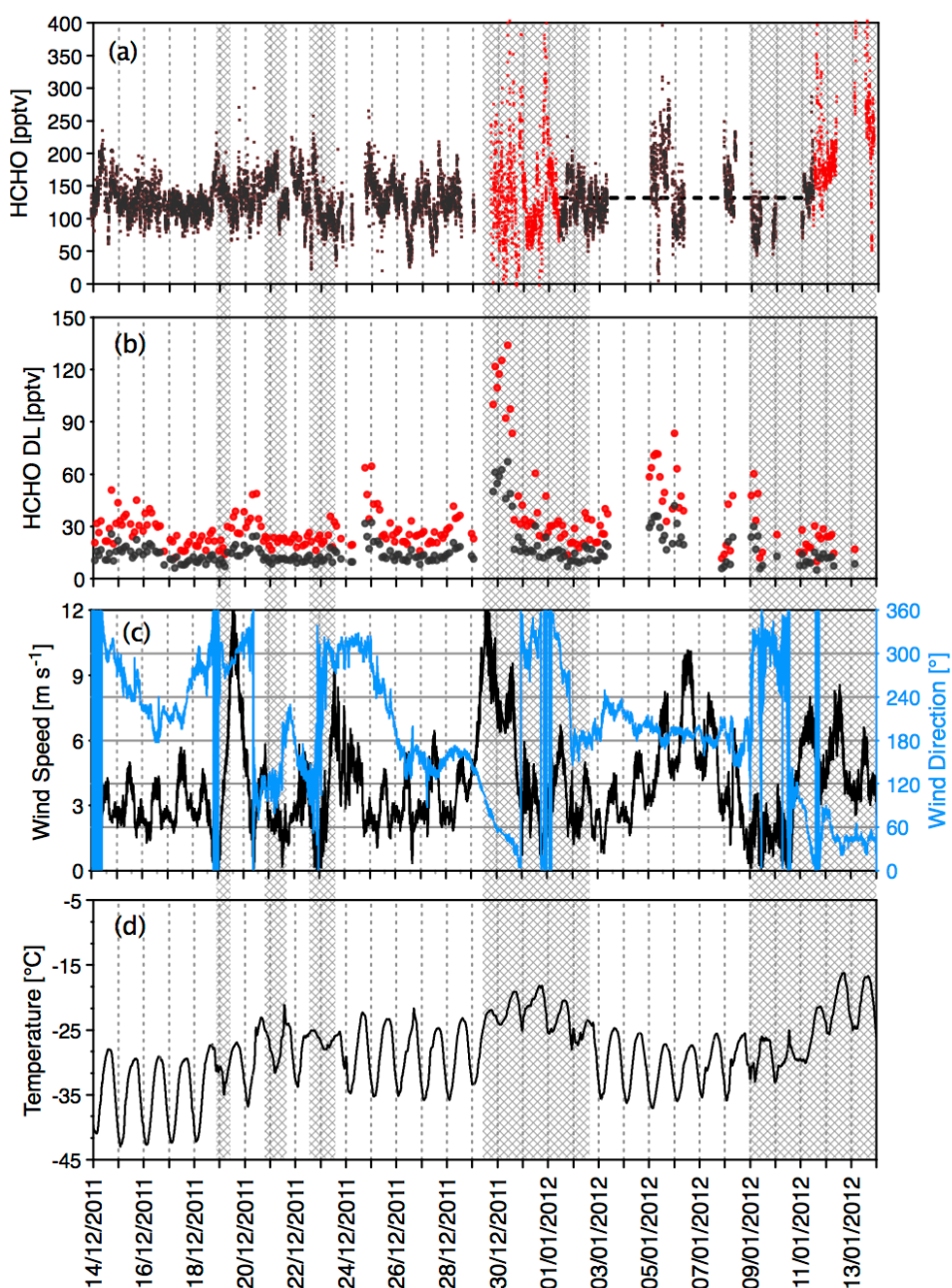


**Fig. 1.** (a) HCHO mixing ratios (time interval of 30 s) measured during the 2011/12 OPALE campaign at 1 m above the snow surface, red points refer to periods during which contamination by wind transport from the station is suspected. The horizontal dashed line indicates the mean mixing ratio observed between January 1<sup>st</sup> and 11<sup>th</sup>, a period over which the sampling was very discontinuous (b) Detection limits (DL), taken as one and two standard deviations of raw zero values measured every two hours. (c) Wind speed and direction. (d) Air temperature. Grey bands denote periods during which clouded sky conditions prevailed.

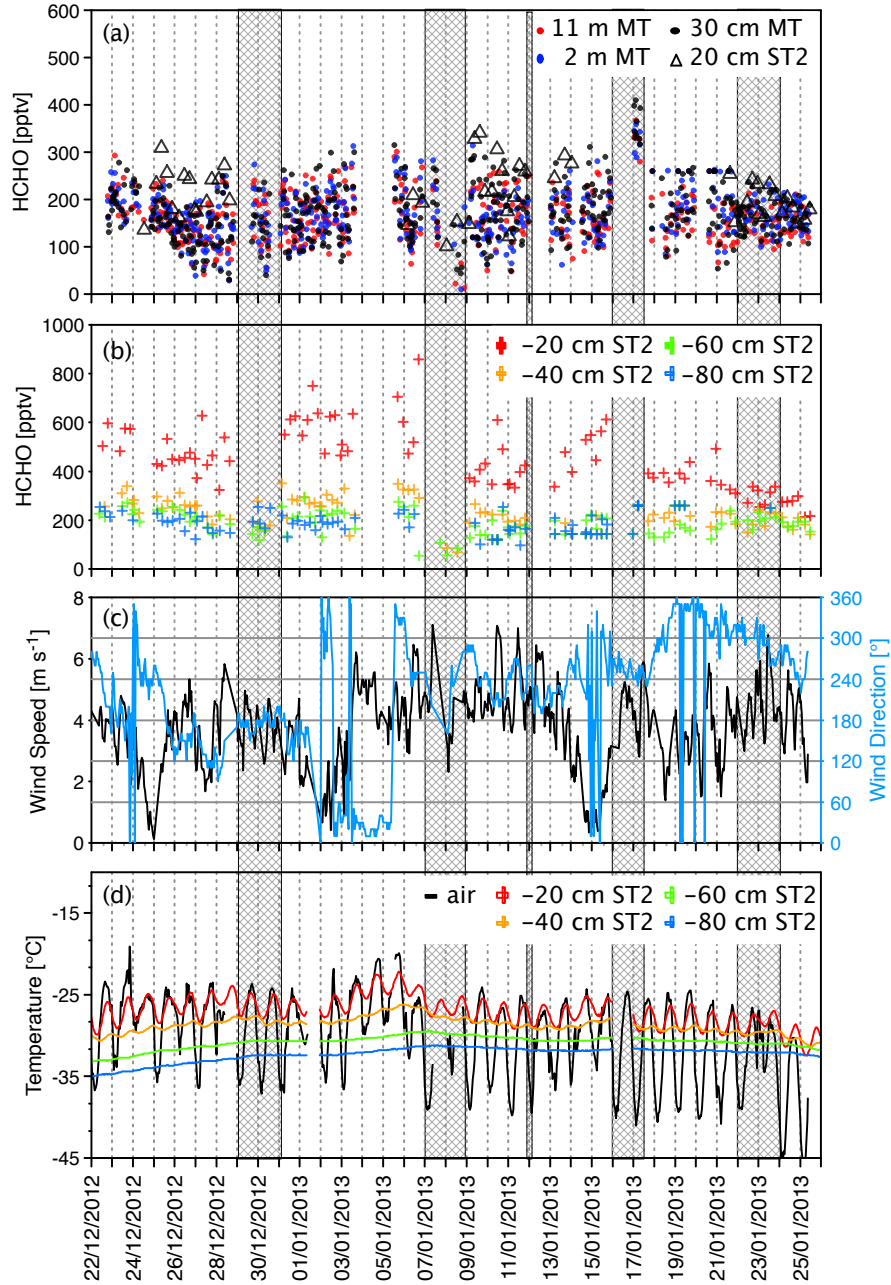
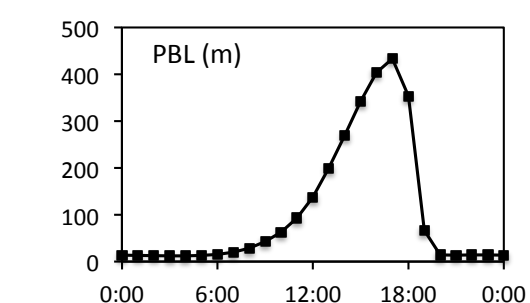
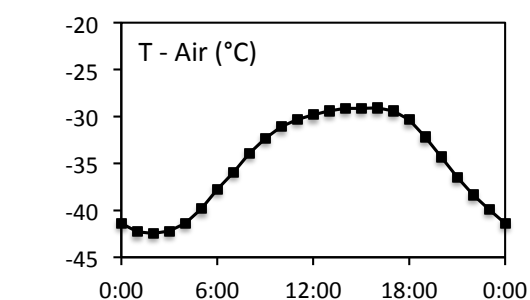
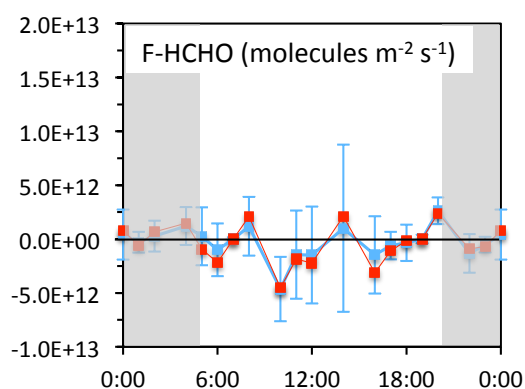
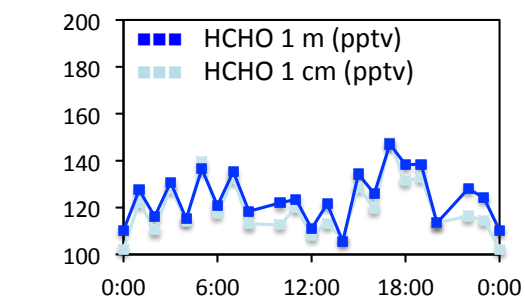


**Fig. 2.** (a) 10 min averaged HCHO mixing ratios observed in the ambient air during the 2012/13 campaign at 3 different heights above the snow on the Meteorological Tower (MT) and at 20 cm on the Snow Tower 2 (ST2) (see Sect. 2.3). (b) 10 min averaged HCHO measured at different depths in the snowpack on ST2. (c) Wind speed and direction. (d) Temperature of air and in snow at different depths (ST2). Grey bands denote periods for which data were not considered due to technical problems of the analyzer and/or the snow tower system. They separate the 6 time intervals over which data were averaged.

2011/12

14.12.2011 - 18.12.2011



2011/12

19.12.2011 - 28.12.2011

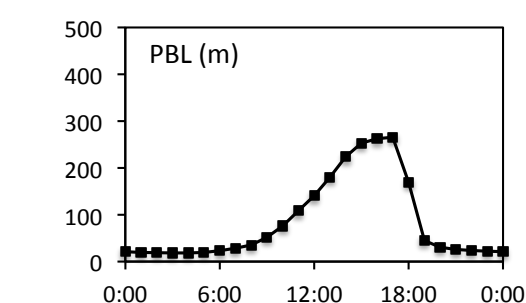
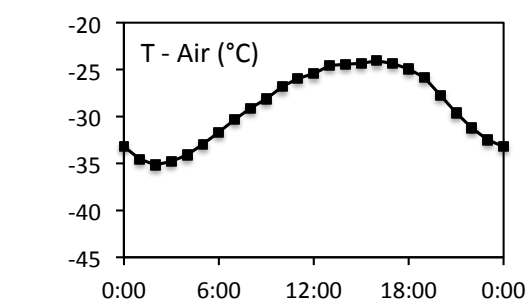
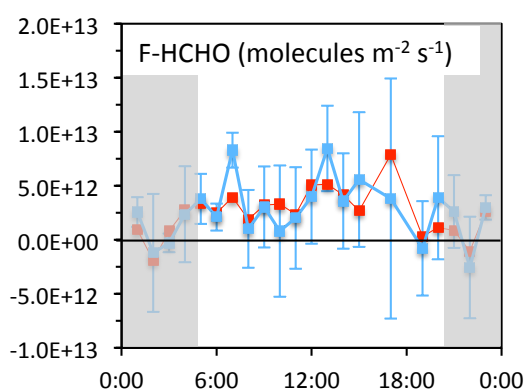
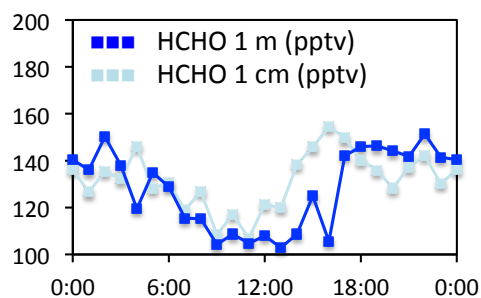


**Fig. 3.** From top to bottom: Mean daily course (hours are in LT) of HCHO mixing ratios measured at 1 m and 1 cm above the ground, snow to air fluxes calculated from observed vertical gradients between 1 m and 1cm (arithmetic means in blue, median values in red), measured ambient air temperatures at Concordia, and simulated PBL heights.

1

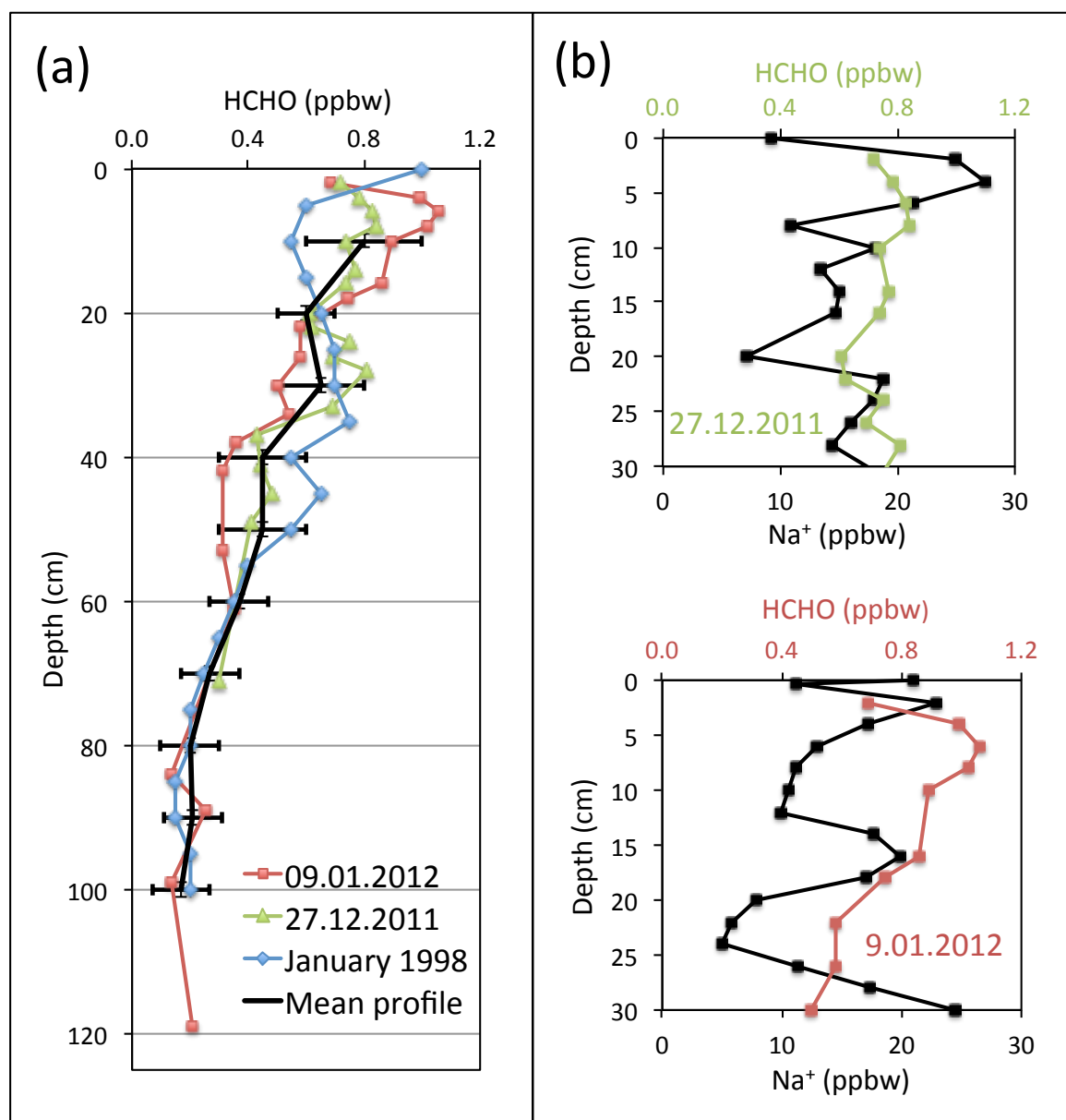
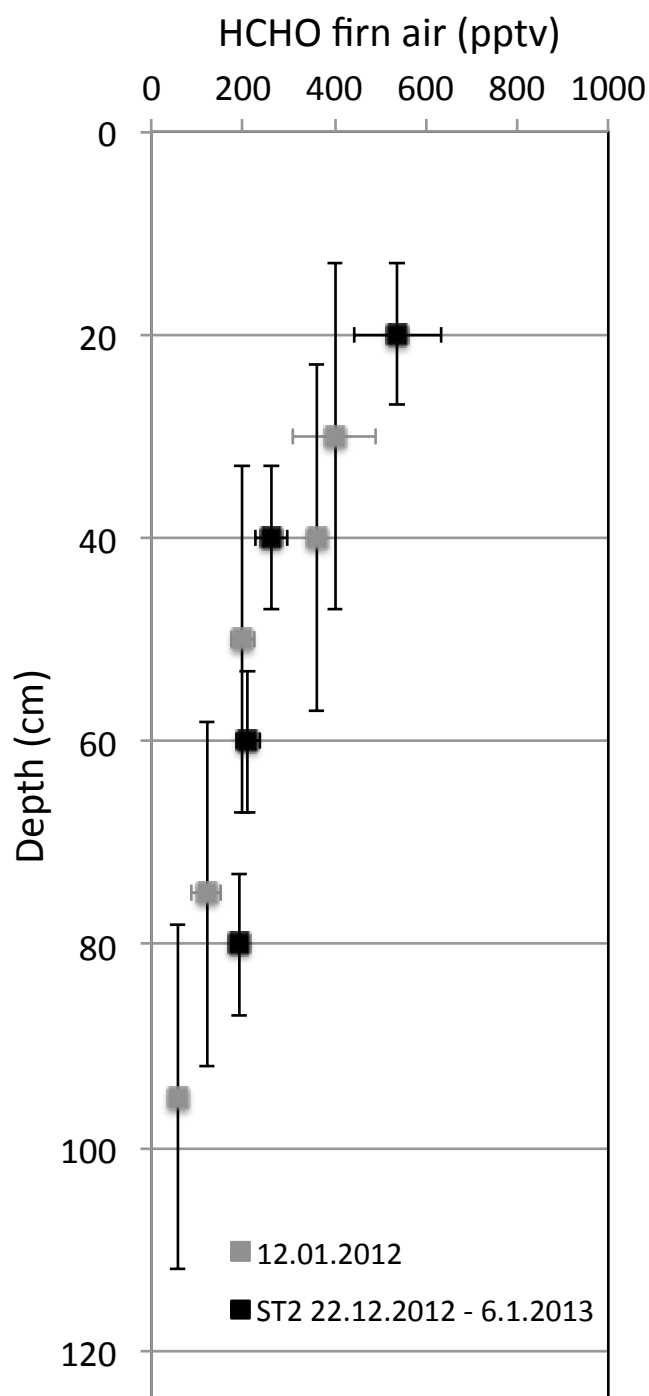


**Fig. 4.** (a) Vertical profiles of HCHO in bulk snow at Concordia. The vertical snow profiles of HCHO obtained from the two snow-pits dug during the 2011/12 campaign are compared to those from a snow-pit dug in January 1998 (Hutterli et al., 2002). (b) Sodium versus HCHO content in the upper 30 cm of the two snow-pits dug in 2011/2012.

1



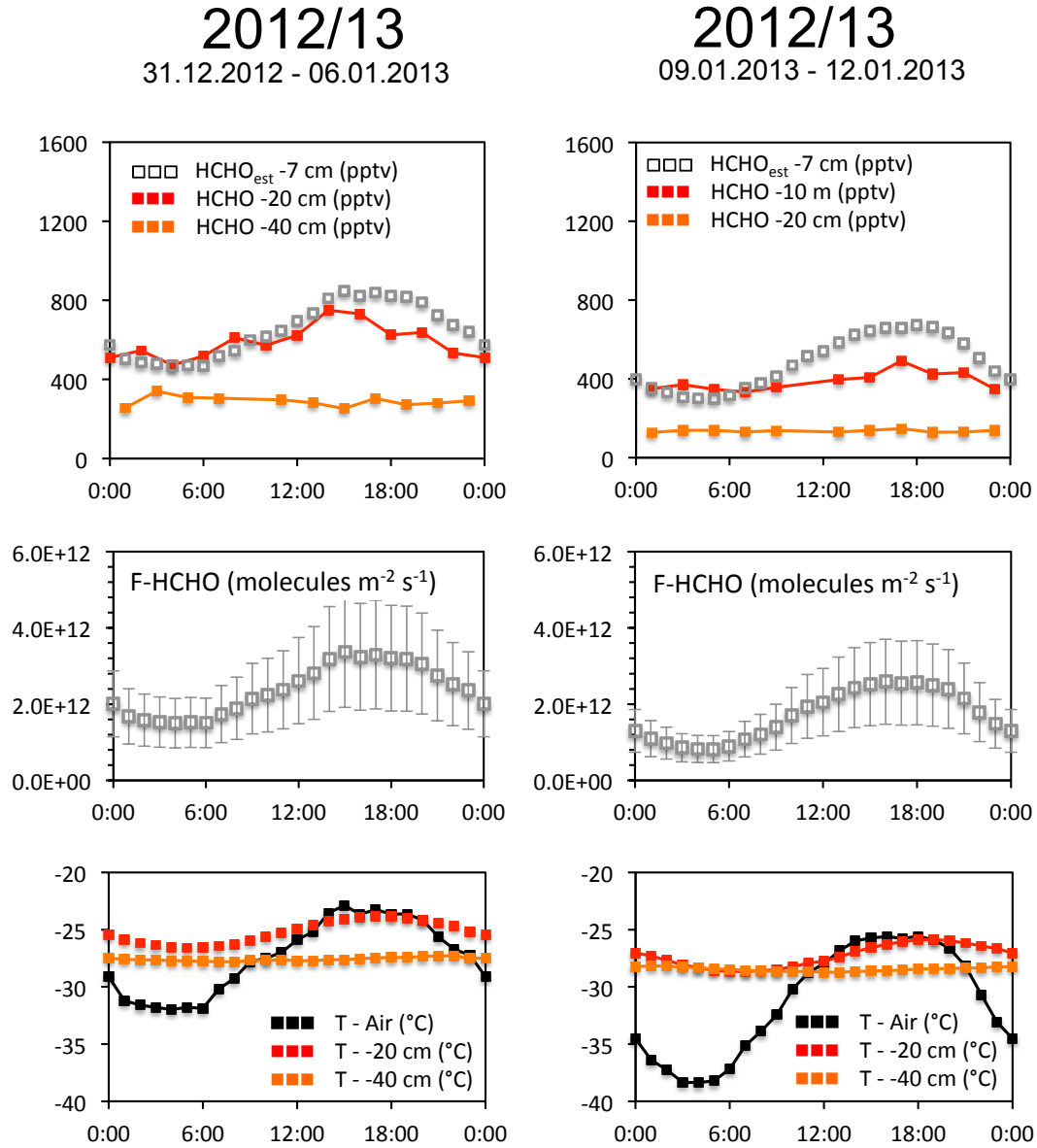
2

3

4 **Fig. 5.** Vertical profiles of HCHO in interstitial air at Concordia. Vertical bars refer to the  
 5 depth from which 66% of air was sampled (see Sect. 2.3) and the horizontal ones to standard  
 6 deviations of 10 min and 30 s means for 2012/2013 and 2011/12, respectively.

7

1  
2  
3  
4

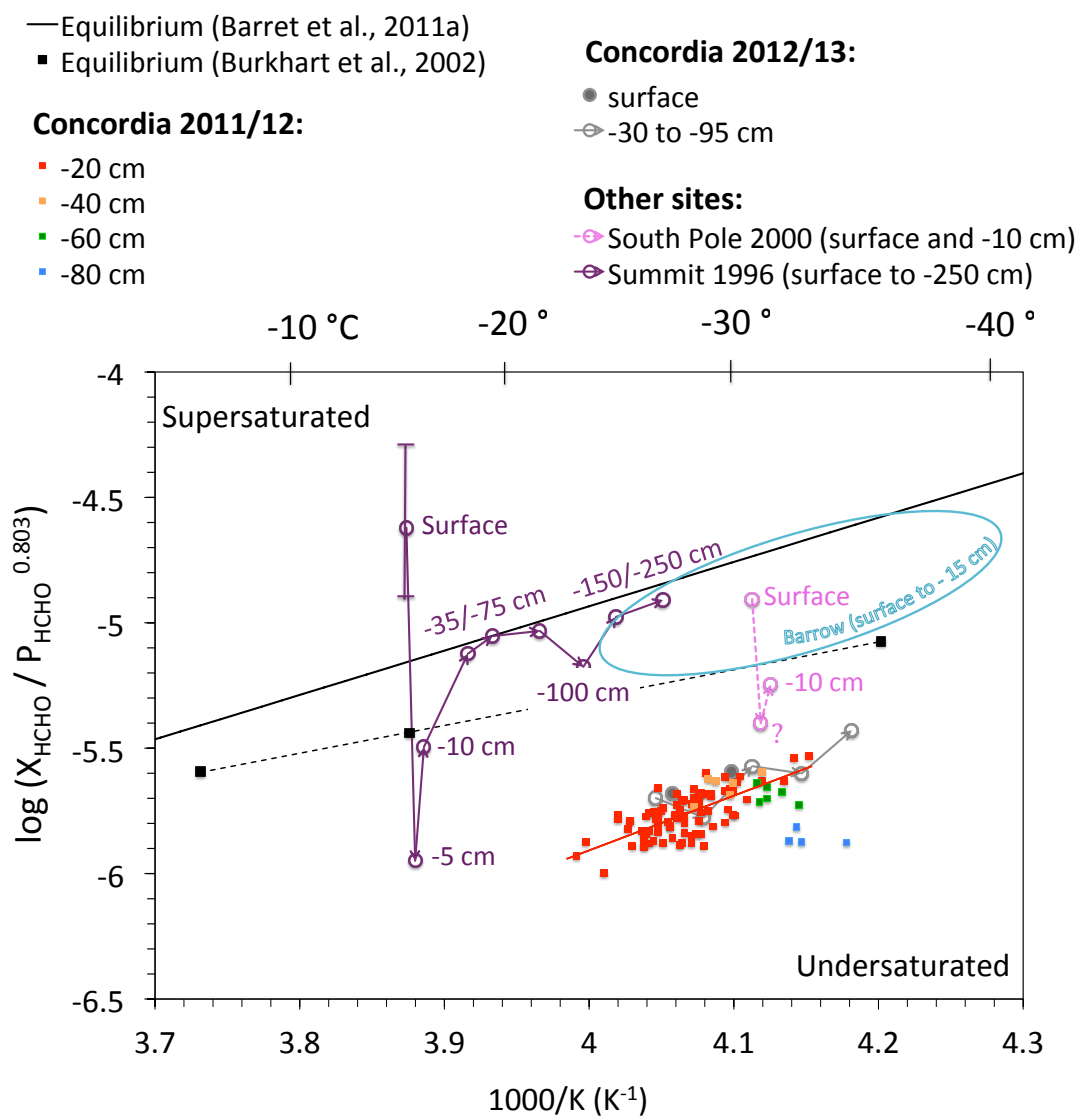


5  
6  
7  
8  
9  
10  
11  
12

**Fig. 6.** Top: Mean daily course (hours are in LT) of firm air HCHO mixing ratios at different depths. At 7 cm below the snow surface, HCHO mixing ratios were estimated. Second from top: HCHO flux calculated from firm air atmosphere gradients. Error bars refer to uncertainties in depth ( $\pm 3$  cm) and in snow concentration ( $\pm 0.08$  ppbw) (see text in Sect. 3.3). Bottom air and firm air temperatures.



1  
2  
3  
4



5  
6 **Fig. 7.** Arrhenius plot of the partitioning coefficient  $K(T)$  for HCHO in firn air and snow of  
7 Concordia, South Pole, Summit and Barrow versus  $T^{-1}$ . The thermodynamic equilibrium as  
8 estimated by Barret et al. (2011a) is reported as black line. Barrow data, which use however  
9 ambient air and not firn air measurements, are situated in the blue ellipse (Barret et al.,  
10 2011b). See discussion in text. Summit snow temperatures were calculated after (Jun et al.,  
11 2002).

12



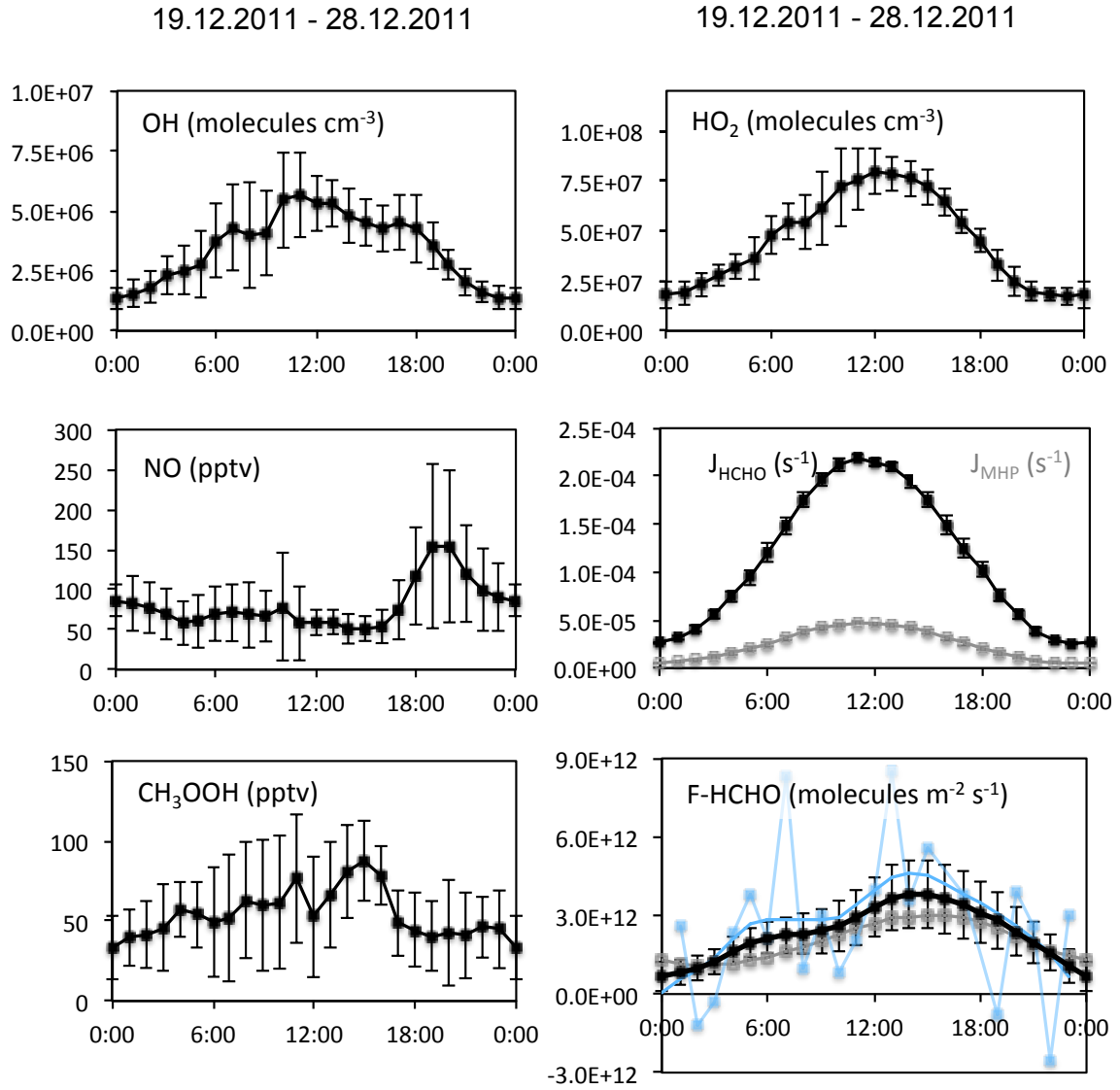


**Fig.8.** Diurnal cycles (hours are in LT) of key input parameters used in 1-D simulations discussed in Sect. 6.  $J_{\text{HCHO}}$  denotes the sum of  $J_{\text{HCHO-mol}}$  and  $J_{\text{HCHO-rad}}$  (see Table 1). HCHO fluxes (F-HCHO) used in the model were taken as the mean (black dots) of F-HCHO derived from atmospheric HCHO gradients (blue dots) and from those derived from firm air atmosphere gradients (grey dots). Vertical bars refer to daily variability and to the uncertainty of calculations in the case of F-HCHO, respectively. OH and HO<sub>2</sub> data are from Kukui et al. (2014), NO from Frey et al. (this issue).

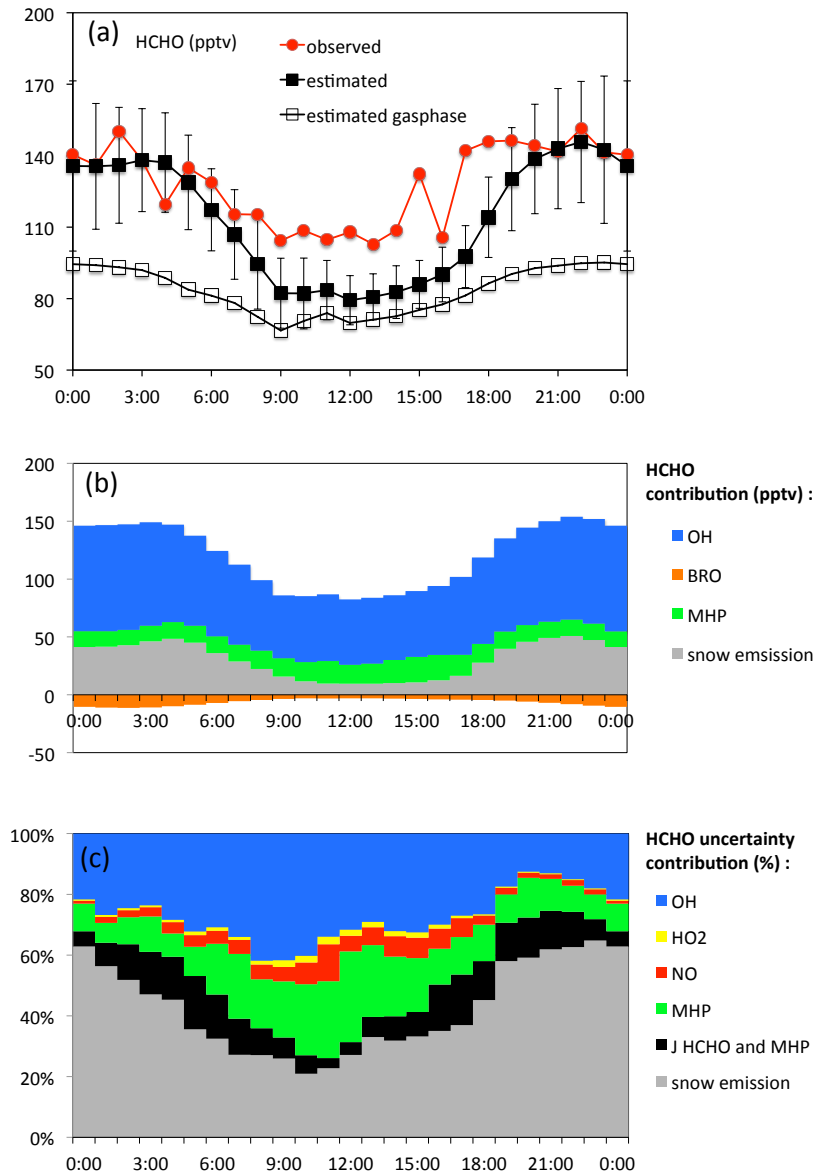


**Fig. 9.** Diurnal cycles (hours are in LT) for the period from December 19<sup>th</sup> to December 28<sup>th</sup> 2011 of: (a) HCHO simulated (squares) and observed (red circles) mixing ratios, grey open squares refer to values simulated when only the gas phase chemistry is considered whereas solid black squares refer to values simulated when both gas-phase chemistry and snow emissions are considered (see Sect. 6). The vertical bars reported on simulated values correspond to uncertainties related to the daily variability and calculation uncertainties of parameters reported in Fig. 8. (b) Simulated HCHO contributions of the different gas-phase

- 1 mechanisms. (c) Contribution of the different uncertainties making up the vertical error bars
- 2 in (a).